Numerical time perturbation and resummation methods for nonlinear ODE

Cynthia Tayeh, Gregory Girault, Yann Guevel, Jean-Marc Cadou

Numerical time perturbation and resummation methods for nonlinear ODE

C. Tayeh, G. Girault, Y. Guevel, J. M. Cadou

Abstract In this research work, numerical time perturbation methods are applied on nonlinear ODE. Solutions are sought in the form of power series using time as the perturbation parameter. This time integration approach with continuation procedures allows to obtain analytical continuous approximated solutions. Asymptotic Numerical Method and new resummations techniques of divergent series namely Borel–Padé–Laplace and Inverse Factorial series are studied. A comparison with classic integration scheme is presented in order to evaluate the robustness and the effectiveness of these algorithms. Full details are given regarding first- and second-order derivative of resummation techniques.

Keywords Time perturbation methods · Numerical resummation · Borel–Laplace · Inverse factorial series · Nonlinear ODE

1 Introduction

Time integration methods, used to solve dynamic problems, rely on a temporal discretization of the problem by advancing the model in successive discrete time steps Δt. However, some constraint can appear especially when resolving nonlinear dynamic problems. One may cite the delicate essential choice of an optimal time step Δt that usually causes the increase in the number of iterations and the computation time. Moreover, it is also shown that classic time integration methods lead sometimes to a destruction in the invariance properties of physical phenomena.

Linear problems have been solved using time perturbation methods in [1]. Hence, for a decade, a time integration scheme based on the perturbation theory is proposed [2]. This makes it possible to overcome the notion of discrete time step. It is connected to a developing area of research that deals with nonlinear problems called the Asymptotic Numerical Method and denoted by "ANM".

This latter is based on the perturbation theory and has been applied with success to various solid and fluid mechanics problems in [3–10]. Recently, time perturbation methods have been studied in [1, 11–13] on some examples. The main idea of this time perturbation technique is to represent the unknowns of the problem in the form of a polynomial by taking the time as the perturbation parameter. Therefore, an analytical approximation of the solution is then valid on a temporal domain to be determined. A continuation technique is then applied to reach a specific final time. The most important advantage of this time approach is that the computed solutions are obtained in a continuous way. However, its main drawback is that the time-series solutions that appear in physics are generally divergent [14–17].

C. Tayeh · G. Girault · Y. Guevel (✉)· J. M. Cadou
UMR CNRS 6027, IRDL, Université Bretagne Sud, 56100 Lorient, France Y. Guevel
e-mail: yann.guevel@univ-ubs.fr

G. Girault
Centre de Recherche des Écoles de Saint-Cyr Coëtquidan, Écoles de Coëtquidan, 56381 Guer Cedex, France

Very recently, a new class of analytic transient solvers with numerical resummation of divergent series has been proposed [2]. Within this new class of temporal integrator, the algorithm that interests us is named Borel–Padé–Laplace and is denoted by "BPL". This type of solver is promising in order to make the numerical simulations more efficient in terms of capture of fast dynamic phenomenon and numerical stability over a large number of cycles and computation time. This algorithm has been successfully applied on academic examples such as the resolution of the heat equation, Burgers equation and some examples of Hamiltonian systems [2,12,13,18–20]. While numerical results have shown that BPL algorithm presents some interesting properties, there are also many disadvantages that need to be alleviated. One may cite the appearance of some numerical poles that can arise with the use of the Padé approximant. Therefore, in such cases, the Borel sum converges very slowly. In order to avoid these problems, another numerical resummation method namely Inverse factorial series and denoted by "IFS" is proposed as a time integration scheme in [21]. A first study on the effectiveness of the Inverse factorial series scheme has been initiated on some academic examples only in [12,21].

Since time perturbation and numerical resummation methods are very recent, our goal is to understand more the behavior and the feasibility of such integration, then develop the way of their use on more complex problems, and finally test their relevance and their robustness.

In this article, we seek to validate the time perturbation and resummation methods on different examples of nonlinear ODE. Details will be presented only for the Van der Pol oscillator problem. It should be noticed that power series solutions for Van der Pol oscillator have been presented in many detailed studies in the literature, for example in [22–26]. In such studies, μ is the perturbation parameter. Whereas in this paper, time is used as the perturbation parameter. It makes it possible to perform a time integration of the problem.

An external force can be simulated as acting on the system by adding a new periodic force to the second member of the Van der Pol equation [27]. This forced equation is studied in some papers [28–33]. Therefore, a study of second member alone is realized by comparing Taylor method and time perturbation methods using some change of variables. This series representation is then used in order to study the full forced Van der Pol equation by time perturbation methods and resummation techniques.

Next, the proposed techniques are applied on the nonlinear combustion equation, then to the hardening spring problem. At the end, the efficiency of these latter is also established for the three degrees of freedom (3 DOF) Lorenz system. Solutions are obtained in a continuous way, which permit to overcome the notion of critical time step Δt related to the condition of Courant–Friedrichs–Lewy (CFL). Since we have no information in advance about the type of numerical series terms obtained, resummation techniques BPL and IFS are also applied. The purpose of this study is to evaluate the recent tools of time perturbation and resummation techniques on these interesting examples. For a fair comparison: the first-, third- and fourth-order accurate Runge–Kutta (RK) method are considered.

This article is structured as follows. In Sect. 2, a brief recall of the numerical time perturbation and resummation methods is exposed. In Sect. 3, these latter are studied and applied in details to the free Van der Pol oscillator, then to the forced Van der Pol in Sect. 4. Next, the advantages of the proposed methods with respect to the classical integration schemes are shown through two examples in Sects. 5 and 6. At the end, the efficiency of these latter is also confirmed for the three degrees of freedom (3 DOF) Lorenz system in Sect. 7.

New estimates of first and second derivatives of Borel–Padé-Laplace and Inverse factorial series, which can prove useful also in other cases of studies to apply the continuation technique, are established and given explicitly in "Appendix A" and "B".

2 Time perturbation and resummation methods

This section consists of a brief recall on the numerical time perturbation and resummation methods. The organization of this section is as follow. First, ANM with time series development is presented in subsection 2.1. Then, the resummation methods Borel–Padé–Laplace and Inverse-Factorial Series are exposed, respectively, in Sects. 2.2 and 2.3.

2.1 Asymptotic numerical method using time as perturbation parameter

Consider the following ordinary differential problem:

$$M\ddot{u} + C\dot{u} + Ku = 0 \tag{1}$$

with the initials conditions at a given time t_0

$$\begin{cases} u(t_0) = u_0 \\ \dot{u}(t_0) = u_1 \end{cases} \tag{2}$$

where M, C and K are prescribed scalars. In the case of multiple degrees of freedom, those quantities are matrices and u,$\dot{u}$, $\ddot{u}$ are vectors.

Unknowns of the problem are sought as truncated power series. In this work, time is the perturbation parameter. Global time is then defined using a given time t_0 and a perturbation time $\hat{t}$ as:

$$t = t_0 + \hat{t} \tag{3}$$

Continuous approximation $u(t) \approx \hat{u}\left(\hat{t}\right)$ writes as follow:

$$\hat{u}\left(\hat{t}\right) = u_0 + \sum_{i=1}^{N} u_i \hat{t}^i \tag{4}$$

where N denotes the truncation order. It is then possible to differentiate this expression as:

$$\dot{\hat{u}}\left(\hat{t}\right) = \sum_{i=1}^{N-1} i u_i \hat{t}^{i-1} \tag{5}$$

$$\ddot{\hat{u}}\left(\hat{t}\right) = \sum_{i=2}^{N-2} i(i-1) u_i \hat{t}^{i-2} \tag{6}$$

These developments are injected into Eq. (1) and by identifying the terms according to the powers of $\hat{t}$, a cascade of linear problems is obtained.

$$\begin{cases} \hat{t}^0 & : 2Mu_2 + Cu_1 + Ku_0 = 0 \\ \hat{t}^1 & : 6Mu_3 + 2Cu_2 + Ku_1 = 0 \\ \hat{t}^2 & : 12Mu_4 + 3Cu_3 + Ku_2 = 0 \\ & \vdots \\ \hat{t}^{N-2} & : MN(N-1)u_N + C(N-1)u_{N-1} + Ku_{N-2} = 0 \end{cases}$$

Series are obtained by the numerical resolutions of those systems. Solutions are then defined on a specific range of validity $[0, t_{\max}]$. An explicit expression of $t_{\max}$ has been proposed in [34]:

$$t_{\max} = \left(\delta \frac{||u_1||_2}{||u_N||_2} \right)^{\frac{1}{N-1}} \tag{7}$$

where δ denotes a given tolerance and $\|.\|_2$ is the Euclidean norm. Note that other definitions to evaluate the range of validity domain exist in [34,35]. As solutions are continuous in time, they can be evaluated at any time $\hat{t} \in [0, t_{\max}]$.

In order to compute solution on a given time range, a continuation algorithm is performed. It can be summarized as follows:

1. Compute series until a given order N.
2. Evaluate the upper bound of the validity domain $t_{\max}$ using δ.
3. Evaluate a new starting point u_0 at a new $t_0 = t_0 + t_{\max}$, and go to 1.

This time series development allows to obtain a numerical approximation of the solutions continuous in time.

2.2 Borel–Padé–Laplace

Drawback of the ANM approach with time as the perturbation parameter is that series might be divergent. In such case, the range of validity of this representation, in the temporal domain, becomes extremely small. Therefore, classical continuation is no longer efficient. To mitigate this difficulty, a new class of analytic transient solvers with numerical resummation of divergent series has been proposed [2,20].

Within this new class of temporal integrator, the numerical algorithm named Borel–Padé–Laplace (BPL) is presented in this subsection. First, a theoretical reminder of Borel–Laplace is quickly presented. The reader is referred to [17,36–39] for more details concerning the definition of Borel resummation method. Then, the numerical algorithm of Borel–Padé–Laplace is exposed.

The first step, after computing the series terms, is to compute the Borel transform given by

$$\mathbb{B}\hat{u}(\xi) = \sum_{n=0}^{\infty} \frac{u_{n+1}}{n!} \xi^n \tag{8}$$

The Borel transform $\mathbb{B}\hat{u}(\xi)$ has a nonzero convergence radius if $\hat{u}$ is a Gevrey series.

Note that $\hat{u}$ is a Gevrey series of index k, if there exists two constants $C > 0$ and $A > 0$ such that

$$|u_n| \leq CA^n(n!)^{1/k}, \quad \forall n \in \mathbb{N} \tag{9}$$

The second step consists to prolongate naturally $\mathbb{B}\hat{u}(\xi)$ into an analytical function $P(\xi)$ (here Padé approximants).

The last one presents the Borel sum $S\hat{u}(t)$ by computing the Laplace transform of P along a direction d:

$$S\hat{u}(\hat{t}) = u_0 + \int_{\mathrm{d}} P(\xi)e^{-\xi/\hat{t}}\mathrm{d}\xi \tag{10}$$

which permits to go back to the originally space.

These three steps are translated into the following numerical algorithm BPL. It is organized around the following three stages: Borel transform ($\mathbb{B}$) + Approximation of Padé (P) + Laplace transform ($\mathcal{L}$). We present this algorithm for Gevrey series of index $k = 1$ in a direction $d = \mathbb{R}^+$.

For the first stage, series terms are computed up to an order N, this yields that Borel transform $\mathbb{B}(\xi)$ is of order $N - 1$.

For the second one, an extension of the Borel transform is obtained by establishing an approximation of Padé, which increases the range of validity of the series:

$$P(\xi) = \frac{A_0 + A_1\xi + A_2\xi^2 + \cdots + A_L\xi^L}{1 + B_1\xi + \cdots + B_M\xi^M} \tag{11}$$

where L and M are two integers such that $L+M = N-1$, $A_0, A_1, \ldots, A_L$ and $B_1, \ldots, B_M$ are the coefficients of Padé approximants. In cases of large size problems, it is recommended to use a vector version of Padé [40]. Note that prolongation of Borel transform can be done with different methods other than Padé. The interested reader is referred to [41] for furthers details, but these methods are designed for linear equations.

For the last stage, the Laplace transform is applied to the Padé approximants in order to return to the temporal space, with a Gauss–Laguerre quadrature [42].

Using the following relation

$$P(\xi)e^{-\xi/\hat{t}} = \left(P(\xi)e^{-\xi/\hat{t}}e^{\xi}\right)e^{-\xi} \tag{12}$$

then applying the Gauss–Laguerre quadrature to Eq. (12) yields to

$$S\hat{u}^N(\hat{t}) = u_0 + \sum_{i=1}^{N_G} P(\xi_i)e^{-\xi_i(\frac{1}{\hat{t}}-1)}w_i \tag{13}$$

where ξ_i are the roots of the N_G-th Gauss–Laguerre polynomial, and w_i are the weights.

Applying the following change of variable $\xi = \xi/\hat{t}$, we get:

$$S\hat{u}^N(\hat{t}) = u_0 + \hat{t}\sum_{i=1}^{N_G} P(\xi_i\hat{t})w_i \tag{14}$$

Since the initial series Eq. (4) is truncated up to an order N, and because of the numerical effects, numerical resummation methods are not able to lead the exact solution. Therefore, Borel sum Eq. (14) allows to approximate analytically the exact solution only in a certain time interval. Moreover, the definition of the range of validity $t_{\max}$ of BPL is still not evaluated explicitly. Therefore, a continuation procedure is proposed to reach specific given time t. The continuation of BPL algorithm is carried out using a criterion based on the residual $Res(t)$ defined by

$$\mathrm{Res}(t) = M\ddot{S}(t) + C\dot{S}(t) + KS(t) \tag{15}$$

where $S(t)$ is the Borel sum presented in Eq. (14), $\ddot{S}(t)$ is the second derivative of Borel sum and $\dot{S}(t)$ the first derivative. Those latter should be determined in order to evaluate the residual. These derivatives are established in "Appendix A". This constitutes one of the main contributions of this work. Therefore, the analytical approximations are examined as long as

$$\|Res(t)\|_2 < \epsilon \tag{16}$$

where ϵ is a small positive parameter and $\|.\|_2$ denotes the Euclidean norm. For the next step, we redefine a new starting point $\hat{x}(t_1)$ where $t_1 > t_0$, which corresponds to the end of the step where relation Eq. (16) holds.

2.3 Inverse factorial series

Another method of resummation called Inverse factorial series, denoted by "IFS" was initially proposed in

the context of time perturbation algorithm in [21]. The link between Borel sum and Inverse factorial series is shown in [21].

We call Inverse factorial series $I(\hat{t})$ the following

$$I(\hat{t}) = u_0 + \sum_{n=0}^{\infty} \frac{b_n n! \hat{t}^{n+1}}{(1+\hat{t}) \cdots (1+n\hat{t})} \tag{17}$$

with

$$b_n = \frac{1}{n!} \sum_{k=1}^{n+1} |\mathbb{S}_s(n, k-1)| u_k \tag{18}$$

where $\mathbb{S}_s(n, k)$ denotes the Stirling numbers of the first kind. Note that Eq. (18) is valid for the Borel summable series in a direction $d = \mathbb{R}^+$. Numerically, $I(\hat{t})$ is computed up to $N-1$ order. However, when the truncation order N is large, the problem appears with the numerical explosion of Stirling numbers.

Hence, an equivalent method to evaluate $I(\hat{t})$, proposed in [43], is described. Suppose that $\hat{u}(t)$ is 1-summable in a direction d, with an angle θ with the positive half-axis.

Let $\tau_l = s_l e^{i\theta}$ with $l = (1, 2, \ldots, N)$, where $\{s_1, s_2, \ldots, s_N\}$ is any sequence of complex numbers. Let

$$z = \frac{1}{\hat{t}}, \qquad y = z e^{i\theta} \tag{19}$$

$$a_1 = \frac{u_0}{z}, a_2 = \frac{u_1}{z^2}, \ldots, a_m = \frac{u_{m-1}}{z^m}, \quad m = 1, \ldots, N \tag{20}$$

Note that if the series are summable in the $\mathbb{R}^+$ direction, we have $y = z$ and we will choose $s_l = l$ for $l \geq 1$.

We call Inverse factorial series the following

$$I(\hat{t}) = \frac{1}{\hat{t}} \sum_{n=0}^{N-1} v_{n+1} = z \sum_{n=0}^{N-1} v_{n+1} = z(v_1 + v_2 + \ldots + v_N) \tag{21}$$

where v_n is the nth term of IFS which are calculated using the following recursive algorithm based on

$$v_{n+1}^{(j)} = \frac{\tau_{n-1} v_n^{(j)} + y v_n^{(j+1)}}{y + \tau_n} \quad n \geq 1, \quad j \geq 1, \tag{22}$$

with

$$v_1^{(1)} = a_1 \qquad v_1^{(2)} = a_2 \qquad \ldots \qquad v_1^{(N)} = a_N \tag{23}$$

The terms $v_1^{(1)}, v_2^{(1)}, \ldots, v_n^{(1)}, v_{n+1}^{(1)}$ are the terms of the IFS denoted by : $v_1, v_2, \ldots, v_n, v_{n+1}$.

The continuation of IFS algorithm is carried out using the criterion of the residual $Res(t)$ defined by

$$\text{Res}(t) = M\ddot{I}(t) + C\dot{I}(t) + KI(t) \tag{24}$$

where $\ddot{I}(t)$ is the second derivative of IFS, and $\dot{I}(t)$ the first derivative of IFS. Therefore, the approximations of derivatives of the IFS algorithm are needed for the residual evaluation. This new part is detailed in "Appendix B". Therefore, the analytical approximations are examined as long as

$$\|Res(t)\|_2 < \epsilon \tag{25}$$

where ϵ is a small positive parameter and $\|.\|_2$ denotes the Euclidean norm. For the next step, we redefine a new starting point $\hat{x}(t_1)$ where $t_1 > t_0$, which corresponds to the end of the step where relation Eq. (25) holds.

3 Application on free Van der Pol oscillator

First, we are interested to study the effectiveness of time perturbation and resummation methods on free Van der Pol oscillator problem that has attracted considerable interest of many researchers from a long time, since it models many problems in different areas [44]. The Van der Pol oscillator equation is a dynamic system described by a variable $x(t)$ satisfying the following nonlinear differential equation of the form

$$\ddot{x} - \mu(1 - x^2)\dot{x} + x = 0 \tag{26}$$

with $x(0) = a$ and $\dot{x}(0) = b$ the initial conditions, and $\mu \geq 0$ denotes the control parameter or the coefficient of nonlinearity. Note that the nonlinear behavior of the oscillations depends on μ. Therefore, according to its value, the trajectories have precise characteristics.

For $\mu = 0$, Eq. (26) becomes

$$\ddot{x} + x = 0 \tag{27}$$

this is a simple harmonic oscillator, which has an exact solution for $t_0 = 0$ on the form:

$$x(t) = x(0)\cos(t) + \dot{x}(0)\sin(t) \tag{28}$$

For $\mu \neq 0$, Eq. (26) have no exact solution; therefore, it was first integrated by the classical discretization schemes, in order to compare the efficiency of time perturbation methods to the classical ones.

3.1 Classical discretization schemes

Equation (26) is written as a first-order system of differential equation:

$$\begin{cases} \dot{x} = y \\ \dot{y} = \mu(1 - x^2)\dot{x} - x \end{cases} \tag{29}$$

A convergence study for different time steps Δt between Runge–Kutta of first (RK1) and fourth order (RK4) has been carried out. For sake of simplicity, only results obtained with RK4 are presented for this example. The goal of this comparison is just to get a good approximation of the solution, since it will be the reference solution.

Firstly, constant time step $\Delta t = 10^{-3}$s is chosen for RK4. Secondly, a type of adaptive RK4 has been used as presented in [45]. It computes local error between two solutions obtained after performing two consecutive time steps using step-size Δt and another using only one time step but with a larger step-size $2\Delta t$. The tolerance parameter on local error denoted Δ_0 makes it possible to adjust the step-size.

Initial conditions at a given time $t_0 = 0$ are arbitrarily chosen as $x(0) = 1$ and $\dot{x}(0) = 0$ and the coefficient of nonlinearity $\mu = 2$.

It should be noticed that for every choice of initial conditions, except $\{x(0) = 0, \dot{x}(0) = 0\}$, a unique periodic motion is presented. The uniqueness of this invariant set, the limit cycle, of the non-forced Eq. (26) can be demonstrated by Liénard's Theorem.

The results of numerical integration by Runge–Kutta methods show that the characteristic of the trajectory depends on the value of the coefficient of nonlinearity μ. For small μ, the limit cycle is very nearly circular. For large μ, the limit cycle is no longer nearly circular and is representative of bounded periodic oscillatory behavior.

3.2 Time perturbation series recurrence formula

In this subsection, time perturbation methods and perturbation–resummation methods are applied on the free Van der Pol oscillator. We seek to demonstrate the accuracy of these methods by comparing their results to RK4 and then check their ability on a problem involving significant temporal variations and limit cycles.

The Van der Pol equation is rewritten again

$$\ddot{x} - \mu(1 - x^2)\dot{x} + x = 0 \tag{30}$$

Let the following change of variable

$$z = x^2 \tag{31}$$

This yields to the new quadratic equation

$$\ddot{x} - \mu(1 - z)\dot{x} + x = 0 \tag{32}$$

We first expand $x(t)$, $\dot{x}(t)$, $\ddot{x}(t)$ and the new variable $z(t)$ as a time power series:

$$\begin{aligned} x(\hat{t}) &= x_0 + \sum_{i=1}^{N} x_i \hat{t}^i \\ \dot{x}(\hat{t}) &= \sum_{i=1}^{N-1} i x_i \hat{t}^{i-1} \\ \ddot{x}(\hat{t}) &= \sum_{i=2}^{N-2} i(i-1) x_i \hat{t}^{i-2} \\ z(\hat{t}) &= z_0 + \sum_{i=1}^{N} z_i \hat{t}^i \end{aligned} \tag{33}$$

where N denotes the truncation order of the series. Substitution of the expansion Eq. (33) into Eq. (32) yields to the following sequence problems:

$$\begin{cases} \hat{t}^0 : \; 2x_2 - \mu(x_1 - z_0 x_1) + x_0 = 0 \\ \hat{t}^1 : \; 6x_3 - \mu(2x_2 - 2x_2 z_0 - x_1 z_1) + x_1 = 0 \\ \hat{t}^2 : \; 12x_4 - \mu(3x_3 - 3x_3 z_0 - 2z_1 x_2 - z_2 x_1) + x_2 = 0 \\ \quad \vdots \\ \hat{t}^N : \; (N+2)(N+1)x_{N+2} \\ \qquad -\mu\left((N+1)x_{N+1} - \sum_{i=0}^{N}(N+1-i)x_{N+1-i} z_i\right) \\ \qquad +x_N = 0 \end{cases}$$

Therefore, series terms for $k \geq 2$ are given by the following recurrence formula

$$\begin{aligned} &k(k-1)x_k \\ &= \mu\left((k-1)x_{k-1} - \sum_{i=0}^{k-2}(k-1-i)x_{k-1-i} z_i\right) - x_{k-2} \end{aligned}$$

where

$$z_i = \sum_{j=0}^{i} x_j x_{i-j} \tag{34}$$

Once the series terms are evaluated, range of validity of the perturbed representation Eq. (33) is sought. In this study, two techniques are used. The first is the historical one for ANM, detailed in [34]. It consists into a tolerance between two consecutive truncation order. The range of validity $[0, t_{\max}]$ using a prescribed tolerance parameter δ and for a truncation order N is evaluated using Eq. (7). When using this criterion, the method will be noted ANM(C). In this paper, for the sake of comparison with other perturbation methods, another criterion is used. Residual tolerance is used in order to evaluate this $t_{\max}$. It makes it possible to ensure the quality of the solution. This method is noted ANM(R).

3.3 Numerical results for time perturbation methods

Initial conditions are set to : $x(0) = 1$ and $\dot{x}(0) = 0$, and the coefficient of nonlinearity is fixed in this subsection to $\mu = 2$.

3.3.1 Numerical results of ANM

Behavior of ANM for different truncation orders N, before any continuation procedure, is presented in Fig. 1. It is observed that only a part of the solution is obtained by computing series, even with a big truncation order N.

Then, the continuation technique is used, the truncation order is fixed to $N = 15$ and the tolerance is set to $\delta = 10^{-6}$. Continuation is depicted in Fig. 2. It should be noted that in between each dots on the plot, solutions are continuous. This is one of the main feature of such approach. It also highlights the accuracy of the continuation of the time series, since it presents the same numerical result as RK4.

3.3.2 Numerical results of Borel–Padé–Laplace

Numerical results of the resummation technique Borel–Padé–Laplace (BPL), with the continuation procedure are presented. The Laplace transform is computed

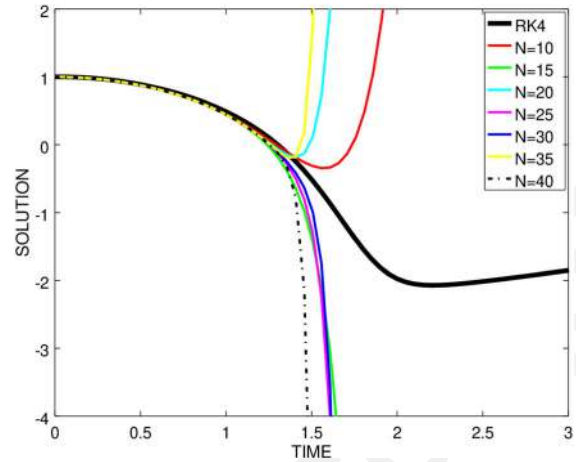

Fig. 1 Free Van der Pol oscillator ANM solutions using different truncation order, and no continuation steps, compared to RK4

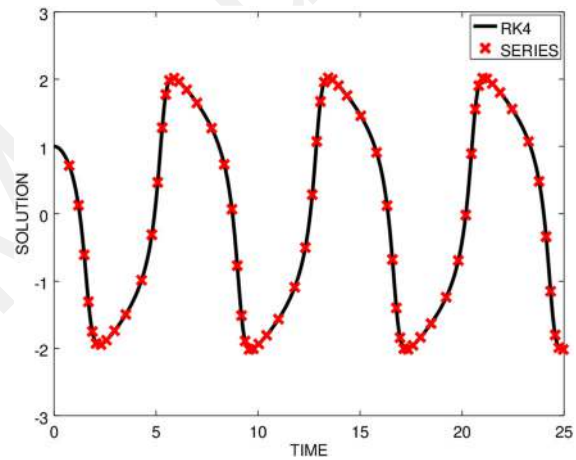

Fig. 2 Free Van der Pol oscillator continuation using ANM series for $N = 15$ and $\delta = 10^{-6}$, compared to RK4

using $N_G = 8$ as number of Gauss points. The real positive axis is the direction of the Laplace transform. Scalar Padé in Eq. (11) applied on Borel's terms are chosen such that: M = integer part $((N-1)/2)$ and $L = (N-1) - M$. The residual is evaluated using the first and second derivative of Borel sum presented in "Appendix A" (in strategy 1). The continuation of BPL based on the residual is carried up to $t = 25\,\mathrm{s}$, $\epsilon = 10^{-4}$.

It can be observed in Fig. 3a that BPL is able to reproduce solutions as RK4. This is further supported by Fig. 3b that shows the ability to reproduce limit cycle.

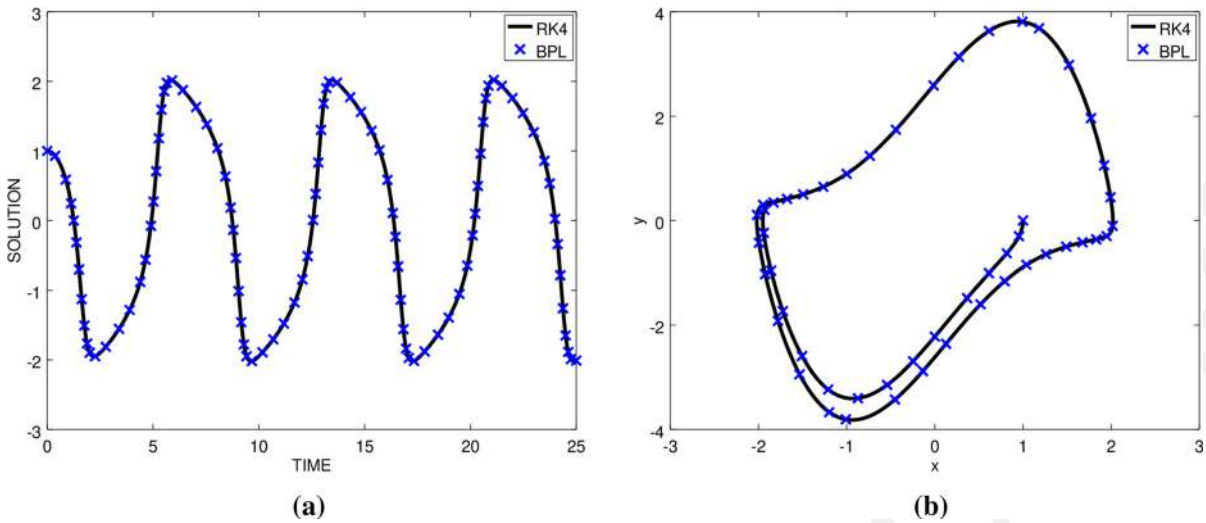

Fig. 3 Approximated solution (left) and phase portrait (right) using BPL for $\epsilon = 10^{-4}$, $N = 15$ for the free Van der Pol oscillator. In black, the reference RK4 solution using $\Delta t = 10^{-3}$s

However, in some cases Borel–Padé-Laplace procedure lacks robustness. For example, apparition of poles resulting from Padé approximants with different examples of parameter changes is depicted in Fig. 4. This might disable efficient continuation procedure.

This drawback is well known. A way to overcome this problem is to use Inverse factorial series resummation algorithm. It is applied also on Van der Pol oscillator, where there is no need to evaluate $P(\xi)$ [see Eq. (11)].

3.3.3 Numerical results of inverse factorial series

We are interested to compute the whole time solution without any difficulty in their representation (as poles with BPL). Therefore, we propose to use IFS for an example of Fig. 4d.

A comparison of the solution by the perturbation method ANM, resummation techniques BPL and IFS for a truncation order $N = 8$ without continuation, is displayed in Fig. 5. Note that IFS algorithm in this paper is using the second method presented in Sect. 2.3.

As expected and per construction, no numerical poles are observed for IFS.

In order to perform continuation procedure using IFS, ranges of validity are using residual norm tolerance. This residual is based on the first and second derivative of IFS presented in "Appendix B". The continuation of IFS based on the residual is carried up to a final time $t = 15$ s, using residual tolerance $\epsilon = 10^{-4}$ and truncation order $N = 8$.

Evolution of the IFS solutions is plotted in Fig. 6. It can be observed that IFS presents the same numerical solution as the classic scheme fourth-order Runge–Kutta. Oscillations with IFS reach also a limit cycle as it can be appreciated in Fig. 6b.

Finally, numerical stability of these numerical schemes has been tested also for a final time $t = 10,000$ s. Numerical results show the ability of time perturbation and resummation methods to reproduce the dynamics of the system over a large time. It should be noted that the long-time behavior of BPL is investigated through numerical experiments on Hamiltonian and non-Hamiltonian system, as well as on a partial differential equations in [20].

3.3.4 Computational efforts

Some global information on computational effort is given in this section. It is noted that the comparison of the performance is not an obvious question in the present study, because solutions obtained by classic or time-perturbation methods are not evaluated in the same way.

To the best of our knowledge, no explicit formula of temporal range of validity of BPL and IFS has been established yet. That is why it is proposed to evaluate it via a residual criterion as in [2]. This latter guarantees

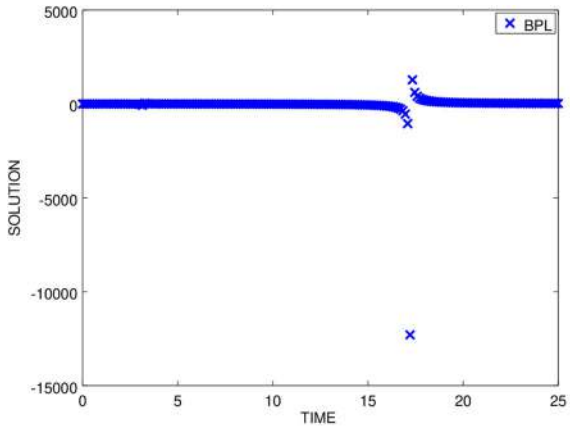

(a) $N = 5, \mu = 2$

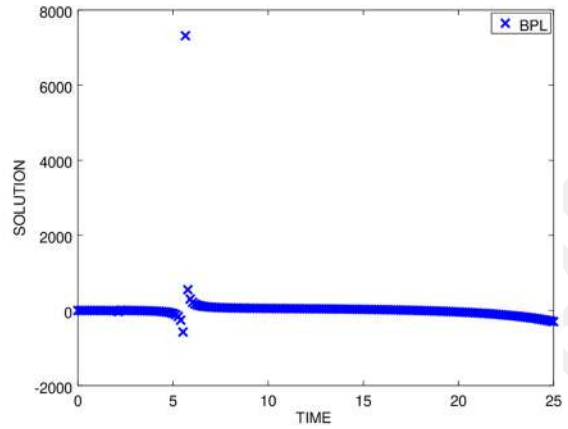

(b) $N = 10, \mu = 2$

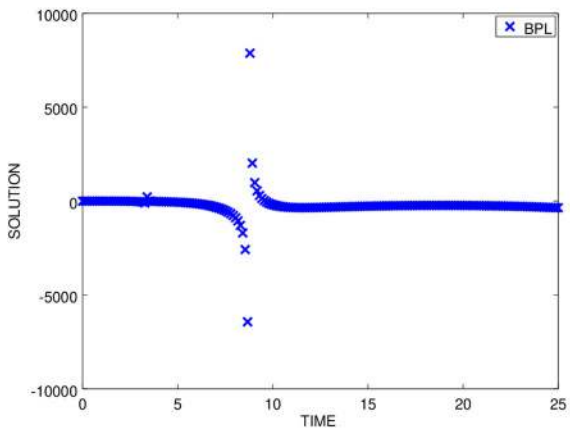

(c) $N = 35, \mu = 2$

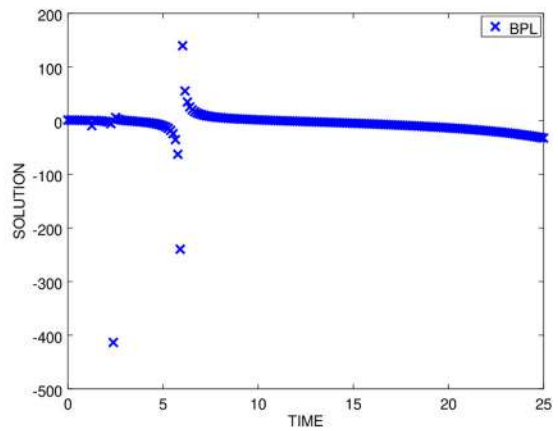

(d) $N = 8, \mu = 2$

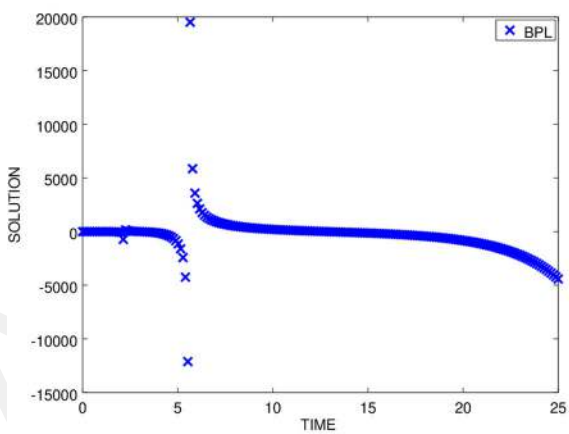

(e) $N = 20, \mu = 8$

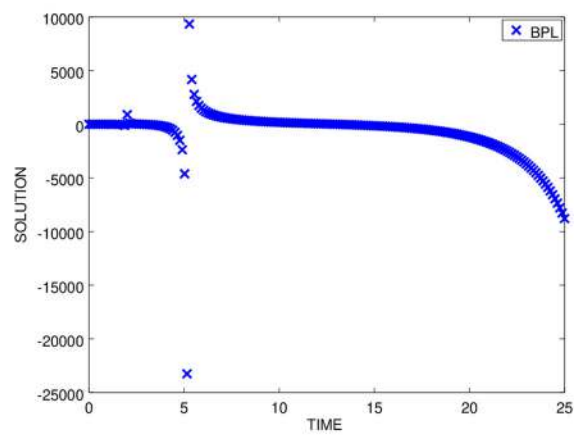

(f) $N = 20, \mu = 10$

Fig. 4 Different examples of apparition of poles resulting from Padé approximant of BPL for the free Van der Pol oscillator

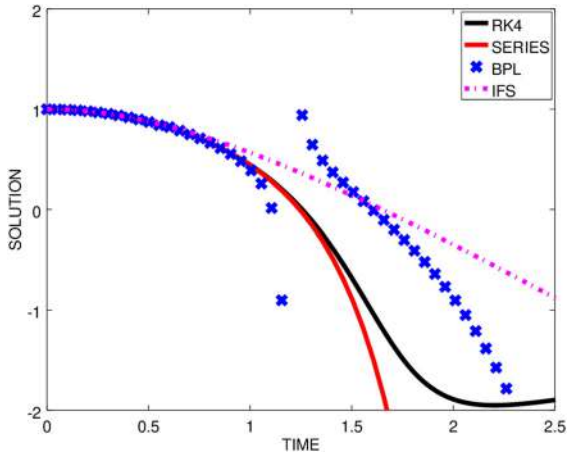

Fig. 5 Approximated solutions obtained using perturbation methods without continuation procedure : SERIES, BPL and IFS, for $N = 8$. In black, the reference curve obtained using classic time stepping RK4 ($\Delta t = 10^{-3}$s)

a very good quality of the solution which is continuous but sometimes time-consuming because of the evaluation of the residue.

We compare the performance of the numerical methods in terms of their computational efficiency, as measured both by computational load (CPU time) and in terms of numerical accuracy as quantified by evaluating the residual of the computed numerical solution.

CPU time needed to reach a final time of $t = 100s$ using RK4 with a constant time step $\Delta t = 10^{-3}s$ is 7.8709 s. Results for RK4 adaptive step size are presented in Table 1 for different values of local error tolerance Δ_0 (Δ_0 denotes the desire accuracy parameter of RK4 as mentioned in [45]).

Table 1 CPU time needed to reach $t = 100$ s using the classic time integration scheme RK4 adaptive time step for different values of local error tolerance Δ_0

Δ_0	CPU time (s)
10^{-3}	0.30296
10^{-4}	0.98494
10^{-5}	3.2892
10^{-6}	10.258

It should be noted that using $\Delta_0 = 10^{-6}$ allows to stay in the same residual range as the perturbation methods.

CPU times for time perturbation techniques are given in Table 2.

ANM(C), based on Cochelin criterion with $\delta = 10^{-5}$ is in the same residual ranges than other methods, allows to reach final time in approximately 0.3s. Interestingly, ANM using a residual norm criterion (ANM(R)) for evaluating tmax and BPL are longer than ANM (C). This shows the problem of using residual for computing range of validity. Finally, it is noted that IFS is relatively less efficient in terms of computational time as can be seen in Table 2.

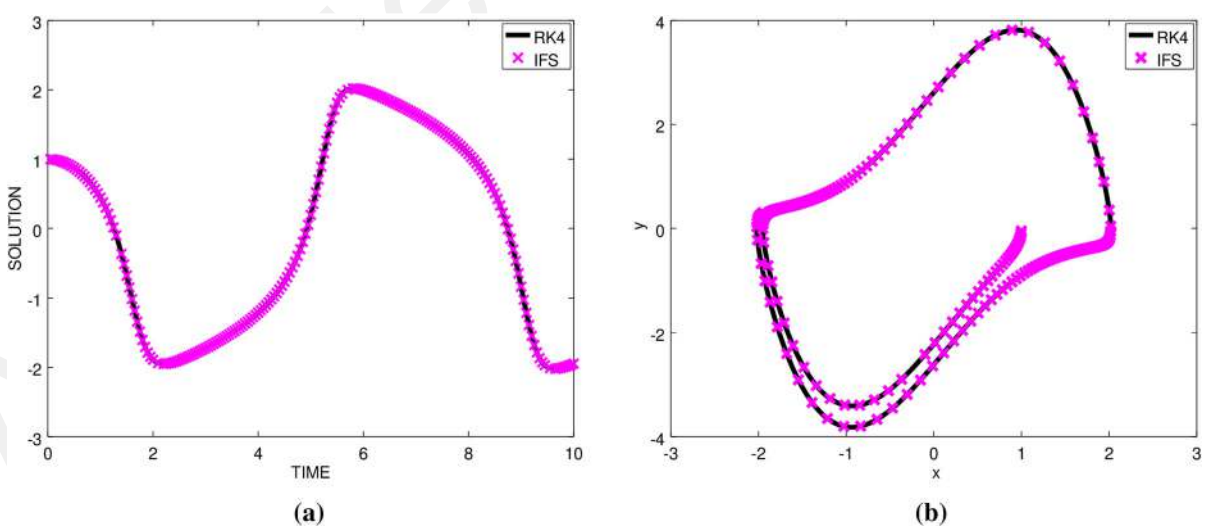

Fig. 6 Approximated solution (left) and phase portrait (right) using IFS for $\epsilon = 10^{-4}$, $N = 8$ for the free Van der Pol oscillator. In black, the reference RK4 solution using $\Delta t = 10^{-3}$s

Table 2 CPU time needed to reach $t = 100\,\mathrm{s}$ time perturbation methods (ANM), time perturbation–resummation methods (BPL, IFS) for a truncation order $N = 8$

Method	CPU time (s)
ANM (C)	0.29951
ANM (R)	1.3056
BPL (R)	3.9281
IFS (R)	7.0321

For time perturbation methods, (R) stands for ranges of validity evaluated using a residual tolerance criterion $\epsilon = 10^{-3}$, while (C) stands for Cochelin criterion using $\delta = 10^{-5}$

So the results show that ANM based on Cochelin criterion with $\delta = 10^{-5}$ is the fastest in CPU time, while the residual stays in the same range as others methods. But when using ANM(C), it is not possible to determine a priori the residual ranges. One have to determine it afterward. One can note that RK4 adaptive step size with $\Delta_0 = [10^{-4}\mathrm{s}, 10^{-3}\mathrm{s}]$ is also fast in CPU time. However, the residual norms of the solution obtained are not as low as the ones prescribed with ANM(R), BPL and IFS.

It is noted that computational efforts of classic and perturbation methods are globally in the same order of magnitude. ANM(C) is 4 time faster than ANM(R). But ANM(R), BPL and IFS ensure a prescribed residual tolerance. Moreover, most of the CPU time is spent in the evaluation of the range of validity. An incremental algorithm is being used, where dichotomy would be much faster. At least, it is possible to conclude that IFS is not so efficient in that case, but might be interesting where BPL is not working due to bad a priori choice of Padé approximants parameters.

3.3.5 ANM, BPL and IFS comparisons

We now propose a comparison of ranges of validity and number of continuation steps needed to reach a specific final time. We recall here that for each continuation step, continuous approximated solutions are obtained using time perturbation methods. For the sake of comparison, ranges of validity are evaluated using the residual criterion.

As a reminder, RK4 needs 10,000 steps to reach a final time of $t = 10\,\mathrm{s}$ using a discrete constant time step $\Delta t = 10^{-3}\mathrm{s}$.

Table 3 Number of steps required to reach $t = 10\,\mathrm{s}$ for the free Van der Pol equation using RK4 adaptive step size with different values of the desire accuracy parameter Δ_0

Δ_0	Number of steps
10^{-3}	177
10^{-4}	575
10^{-5}	1922
10^{-6}	6026

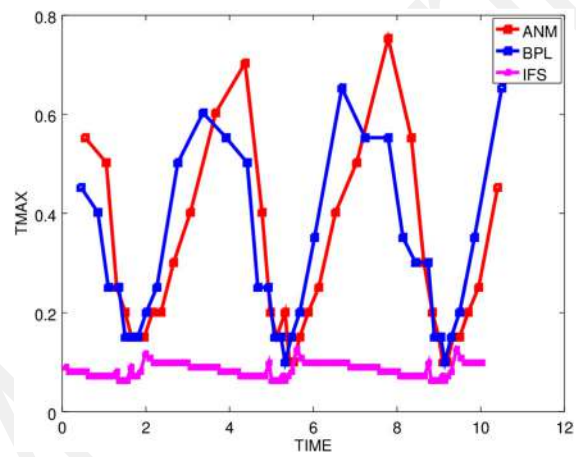

Fig. 7 $t_{\max}$ evolution for ANM, BPL and IFS for $N = 15$, and $\epsilon = 10^{-4}$

A small study on number of step is presented in Table 3 for adaptive RK4 based on [45]. For every Δ_0 value, residual of solutions were globally higher than 10^{-3}.

Evolution of $t_{\max}$ obtained using ANM (Series only), BPL and IFS (numerical resummation) is proposed in Fig. 7. It is observed an automatic adaptation of the range of validity $[0, t_{\max}]$ accordingly to the cyclic solution. Ranges of validity for ANM and BPL oscillate around $0.4s$ and stay bounded in $[0.1, 0.78]s$.

Number of steps for ANM, BPL, and IFS with each other are given in Table 4. It is noted that ANM and BPL reach final time using approximately the same number of steps. BPL is slightly better than ANM in this example. IFS performs two to four times more steps than other methods in this example.

The results of this study highlights the effectiveness of the analyticity of the approximation, since it can represent the important temporal variations in the evolution of the physical phenomenon studied.

Finally, regarding computational efforts and number of steps for adaptive RK4 and time perturbation

Table 4 Case of the free Van der Pol equation. Number of steps needed to reach final time $t = 10\,\mathrm{s}$ using perturbation methods with $N = 15$ and different values of the residual tolerance ϵ

Residual tolerance	ANM	BPL	IFS
10^{-2}	24	21	55
10^{-3}	30	26	79
10^{-4}	36	33	99
10^{-5}	44	41	168
10^{-6}	51	50	214

methods it is possible to say that wider step size is performed, in a slightly better amount of time and for a better prescribed accuracy of the solution.

3.4 Behavior for a higher value of μ

In this subsection, we consider the same equation of the free Van der Pol oscillator by increasing the nonlinearity coefficient μ to 1000. In this particular case, the solution changes radically and presents oscillations on a much longer time scale.

We are interested to see how the polynomial approaches can deal with large values of the nonlinearity coefficient where the equation becomes stiff and some very fast dynamic in the system is expected.

First, Fig. 8 displays the results of the solution obtained by time perturbation method ANM and RK4 for a discrete time step $\Delta t = 10^{-4}$s and for a final time $t = 6000\,\mathrm{s}$. One can see that the solutions are superposed. A zoom of the plot close to the area of fast changes of the solution is presented in Fig. 9. It is observed that ANM solution is different than the one obtained by RK4 with a discrete time step $\Delta t = 10^{-4}$s. For this reason, we decrease the step size to $\Delta t = 10^{-5}$s. With this latter, RK4 solution is now in a good agreement with ANM solution as can be appreciated in Fig. 9.

An additional plot of the velocity in that vicinity of the "jumps" that can give an additional insight in the quality of the approximation is presented in Fig. 10.

As mentioned in [46], if we integrate a stiff problem using variable-step Runge–Kutta, the initial step size chosen generally leads to a large local error estimate. This then causes the routine to reduce the step size, until the main local error is reduced to its specified limit. The routine sometimes works well to integrate the problem,

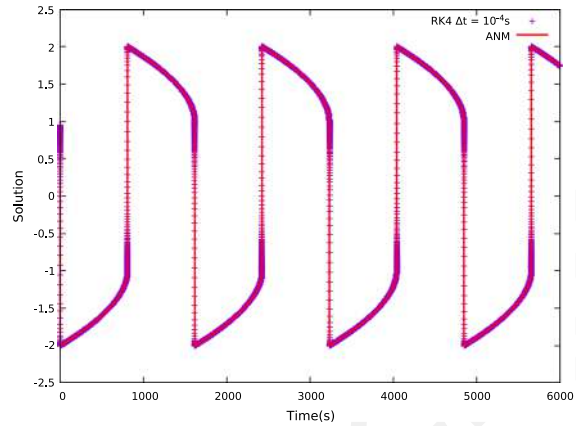

Fig. 8 Approximated solution using RK4 with a discrete time step $\Delta t = 10^{-4}$s, and ANM for a truncation order $N = 15$, for the free Van der Pol oscillator with $\mu = 1000$

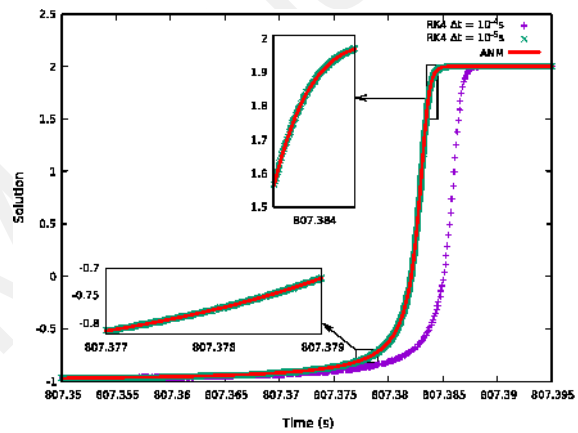

Fig. 9 Enlarged view of Fig. 8 of the approximated solution using ANM and RK4 with two discrete time steps $\Delta t = 10^{-4}$s and $\Delta t = 10^{-5}$s, with $\mu = 1000$

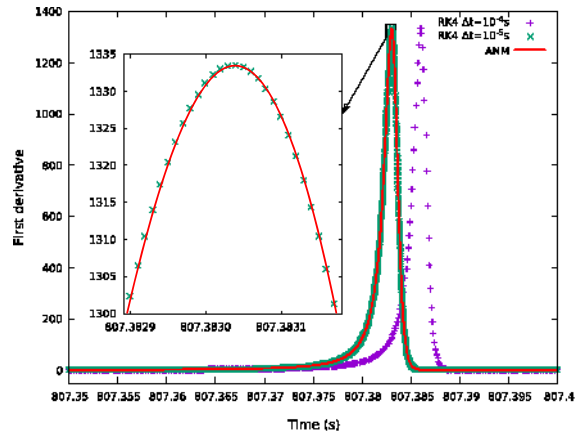

Fig. 10 Zoom plot of the approximated velocity using ANM and RK4 with a discrete time step $\Delta t = 10^{-5}$s, with $\mu = 1000$

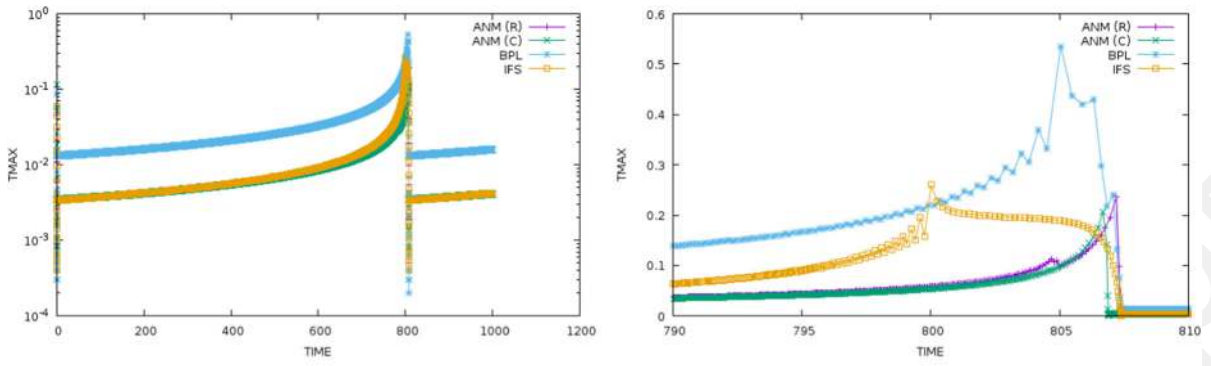

Fig. 11 $t_{\max}$ evolution for ANM(R), ANM(C), BPL and IFS for $N = 25$, $\mu = 1000$. (R) stands for ranges of validity evaluated using a residual tolerance criterion $\epsilon = 10^{-4}$, while (C) stands for Cochelin criterion using $\delta = 10^{-4}$

but uses a much larger number of steps than seems logical. As a result, rounding error and computation time are constraints when using classical techniques to integrate such problems.

These constraints are surmounted with the time perturbation methods. This example is a very good illustration to realize that these methods are also appropriate for stiff problems.

Same results are obtained with the other time perturbation–resummation methods BPL and IFS presented in this work.

We are now interested in comparing the range of validity of these time perturbation and resummation methods. The comparison is carried out in Fig. 11 for a truncation order $N = 15$. It is observed that use of the resummation methods BPL and IFS tend to increase the range of validity of the ANM series in this case.

4 Application on forced Van der Pol oscillator

An external transient force $F(t)$ can act on the oscillator, by placing at the second member a function of t, which is equivalent in mechanics to the actions of an external force on the system :

$$\ddot{x} - \mu(1 - x^2)\dot{x} + x = F(t) \tag{35}$$

This equation is called forced Van der Pol.

The external action will be assumed sinusoidal periodic force; therefore, the second member $F(t)$ is chosen as $A\cos(\omega t)$, where A denotes the forcing amplitude and ω the forcing frequency. While we use time perturbation for the unknowns, this right hand side (RHS) also needs to be represented by a power series. In order to obtain the best numerical solution of the complete forced Eq. (35), it is necessary to have the best approximation of this RHS. Therefore, a time perturbation study of this RHS is realized by comparing Taylor method and time perturbation methods using specific change of variable [47].

4.1 Time perturbation of the forcing term

The chosen time-dependent forcing term is $F(t) = A\cos(\omega t)$. It is necessary to look for a polynomial approximation of it, as:

$$\hat{F}\left(\hat{t}\right) = F_0 + \sum_{i=1}^{N} F_i \hat{t}^i \tag{36}$$

with $F_0 = F(t_0)$. Two specific procedures are compared in order to evaluate the F_i series terms.

4.1.1 Variable change

The following change of variable $U = \cos(\omega t)$ and $V = \sin(\omega t)$ proposed in [47] leads to

$$\begin{cases} U = \cos(\omega t) \\ V = \sin(\omega t) \end{cases} \Longrightarrow \begin{cases} \mathrm{d}U = -\omega V \ \mathrm{d}t \\ \mathrm{d}V = \omega U \ \mathrm{d}t \end{cases} \tag{37}$$

Writing U and V as series : $U = \sum_{i=0}^{N} U_i \hat{t}^i$ and $V = \sum_{i=0}^{N} V_i \hat{t}^i$, then injecting them into Eq. (37),

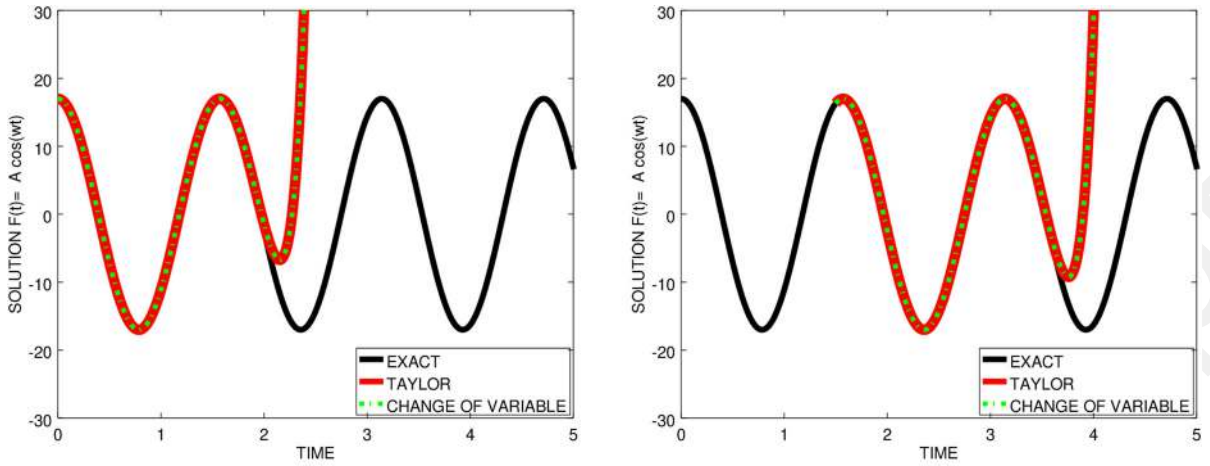

(a) Initial time $t_0 = 0$ **(b)** Initial time $t_0 = 1.5$

Fig. 12 Influence of the initial time t_0 for the time perturbed RHS: $F(t) = A\cos(\omega t)$ without continuation procedure. Comparisons with the exact solution (plain black curve) are performed for $A = 17$, $\omega = 4$ and truncation order $N = 20$

and finally equating terms with identical powers of $\hat{t}$, we get for $i \geq 1$:

$$\begin{cases} U_i = -\frac{\omega}{i} V_{i-1} \\ V_i = \frac{\omega}{i} U_{i-1} \end{cases} \tag{38}$$

The initial terms are $U_0 = \cos(\omega t_0)$ and $V_0 = \sin(\omega t_0)$, where t_0 denotes a given initial time.

Thus, the recurrence formula for the RHS is:

$$F_i = AU_i \quad , \quad \forall i \geq 0. \tag{39}$$

4.1.2 Taylor decomposition

The general formula of Taylor series for $\cos(\omega t)$ also makes it possible to determine the F_i series terms:

$$\cos(\omega t) = \sum_{i=0}^{N} \frac{(\cos(\omega t_0))^{(i)}}{i!} (t - t_0)^i \tag{40}$$

where $(\cos(\omega t_0))^{(i)}$ denotes the ith derivative of the cosine function evaluated at the point ωt_0. This formula has been directly used for numerical validation. Recurrence formula for the F_i terms is not provided here as it was not necessary.

4.1.3 Numerical validation of the RHS series representation

Exact solution is compared to the solution given by Taylor method and the change of variable method, for $A = 17, \omega = 4$. It is done without continuation procedure in order to fully understand the behavior of the obtained series. Firstly, influence of the initial time t_0 is depicted in Fig. 12 using truncation order $N = 20$. No difference can be seen between both methods, nor influence of the initial time. Secondly, truncation order influence is presented in Fig. 13. It can be seen that the domain of validity $t_{\max}$ of the RHS, $\approx 1.5s$, is wider than previously computed branch of solutions.

Numerical results for the zeroth step show that the two methods: Taylor formula and the method based on change of variable have the same behavior, same range of validity and same error with the exact solution. As it is easier to evaluate Eq. (39) than finding a recurrence formula for the Taylor expansion for $t_0 \neq 0$, we decide to use this method for the RHS.

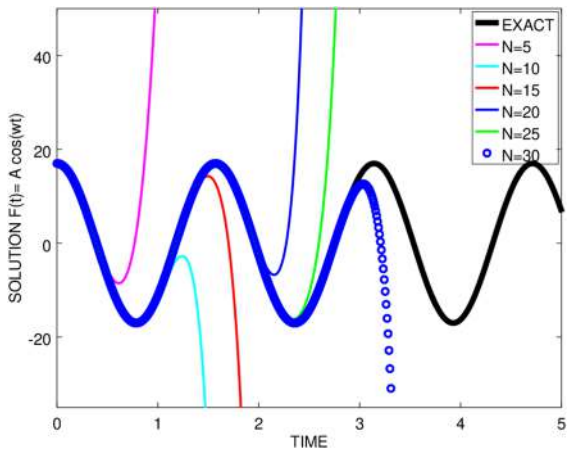

Fig. 13 Influence of the truncation order for the time perturbed RHS $F(t) = A\cos(\omega t)$ without continuation procedure. Comparisons with the exact solution (plain black curve) are performed for different truncation orders N, for $A = 17$, $\omega = 4$ and $t_0 = 0$

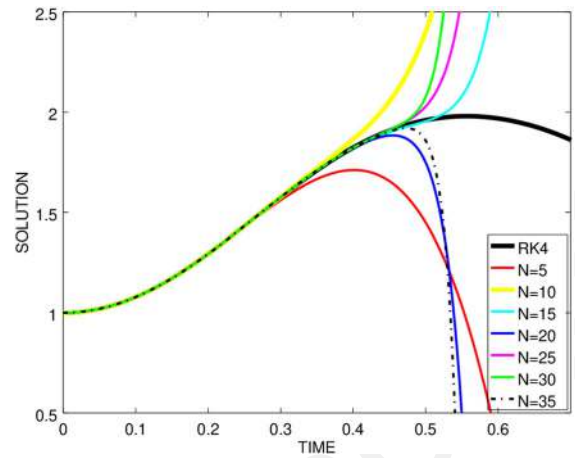

Fig. 14 Approximated solution using ANM (series only) for different truncation orders N, in the case of the forced Van der Pol oscillator ($\mu = 2$, $\omega = 4$ and $A = 17$)

4.2 Numerical study of the forced Van der Pol equation

4.2.1 Classical discretization schemes

The forced Van der Pol equation (35) is solved by converting it into a first-order system of differential equation:

$$\begin{cases} \dot{x} = y \\ \dot{y} = \mu(1 - x^2)\dot{x} - x + F(t) \end{cases} \tag{41}$$

A convergence study for different time steps Δt between RK4 and RK1 schemes has been also carried out in this case. The corresponding time step for $x(0) = 1$, $\dot{x}(0) = 0$ and $\mu = 2$ is $\Delta t = 10^{-3}s$.

4.2.2 Time perturbation representation

In order to solve the forced Van der Pol equation using time perturbation, we proceed with the same procedure as in the free case. Power series representation of the unknowns Eq. (33), using time as the perturbation parameter, are injected in the equation to solve Eq. (35). Moreover, series terms F_i of the RHS are evaluated using Eq. (39). Therefore, identifying the terms according to the powers of $\hat{t}$, the following recurrence formula is obtained:

$$k(k-1)x_k = \mu\left((k-1)x_{k-1} - \sum_{i=0}^{k-2}(k-1-i)\,x_{k-1-i}\,z_i\right) - x_{k-2} + F_{k-2} \tag{42}$$

where

$$z_i = \sum_{j=0}^{i} x_j x_{i-j} \tag{43}$$

4.2.3 Numerical results

For all the computations, initials conditions are set to $x(0) = 1$, $\dot{x}(0) = 0$, the amplitude to $A = 17$ and the frequency to $\omega = 4$.

In order to understand the behavior of the ANM, solutions are plotted without continuation procedure in Fig. 14. It can be seen a standard evolution in perturbation method. After some time, continuous solutions diverge. Moreover, the more terms you add in the representation, the wider is the range of validity.

Solutions and phase portrait are proposed in Fig. 15. Continuation procedure is exactly the same as in the free case. Residual norm tolerance is set to an ϵ value, and this makes it possible to evaluate the range of validity of the time perturbation representation $t_{\max}$. The same results are obtained using IFS and ANM. They are not plotted here for sake of conciseness. Hence, it is confirmed that ANM, BPL and IFS are able to reproduce solutions of the forced Van der Pol equation.

A small robustness study is proposed for the time perturbation methods. Phase portraits are plotted in Fig. 16 for BPL only (but results are the same for ANM and IFS methods). It is done for others values of the forced Van der Pol equation parameters A, ω and μ .

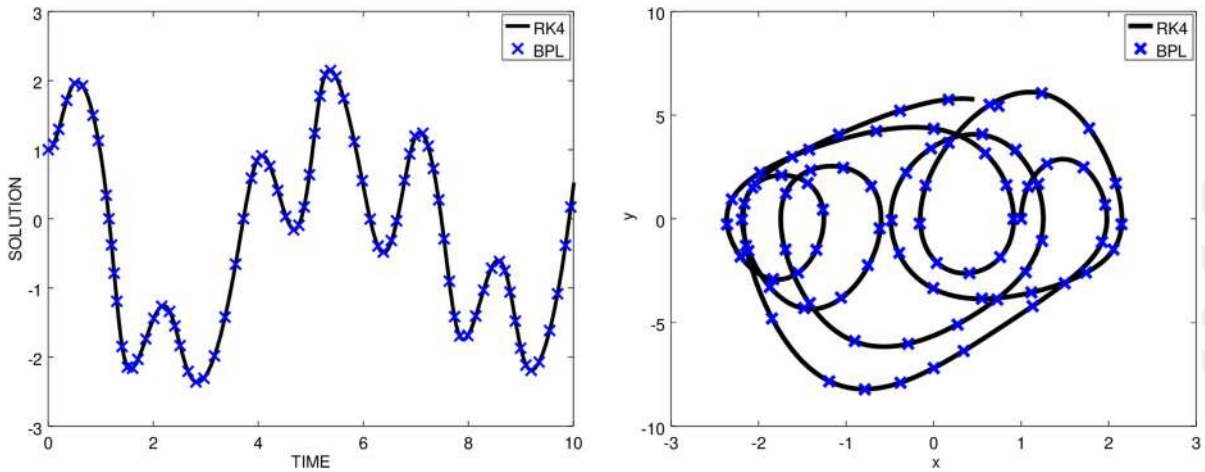

Fig. 15 Approximated solution (left) and phase portrait (right) using BPL for $\epsilon = 10^{-4}$, $N = 15$, $\mu = 2$, $\omega = 4$ and $A = 17$ for the forced Van der Pol oscillator. In black, the reference RK4 solution using $\Delta t = 10^{-3}$s

Perfect agreement with the RK4 solutions is observed. This confirms the ability of the proposed methods to reproduce numerical solutions of the forced Van der Pol oscillator.

Number of steps for ANM, BPL and IFS needed to reach final time $t = 10$ s are given in Table 5. Domain of validities is around 0.1 s to 0.2 s. It is once again recalled that solution within those steps is continuous. Moreover, derivative values are available at any time and are also continuous in time. It is noted that ANM and BPL methods are equivalent in terms of number of steps for this case of study and those parameters. But, it is not easy to find BPL parameters (truncation order, number of Gauss point) for which no pole appears. At last, IFS needs about 50% more steps than BPL and ANM.

5 Application on the nonlinear combustion equation

We now consider a model of flame propagation. If a match is lit, the fireball spreads rapidly until it reaches a critical size. It then preserves this size because the amount of oxygen absorbed by the combustion inside the ball balances the amount accessible through the surface of the fireball. To illustrate this further, let us consider the following nonlinear combustion equation [48]:

$$\dot{y} = y^2(1 - y) \tag{44}$$

with the initial condition

$$y(0) = \delta \tag{45}$$

The scalar variable $y(t)$ represents the radius of the ball. The terms y^2 and y^3 refer to surface area and volume. The critical parameter δ corresponds to the initial radius which is small. The solution is sought over a length of time such that $t \in [0, 2/\delta]$.

This example is studied by Larry Shampine, one of the authors of the MATLAB's suite of ordinary differential equations [49]. This problem is characterized by its transitory aspect in the middle of the integration interval. The solution switches from non-stiff to stiff, and then, it becomes non-stiff again.

Series terms of time perturbation method for Eq. (44) are given in "Appendix C.1".

The exact solution of this differential equation is [50]:

$$y(t) = \frac{1}{W(a\exp(a - t)) + 1} \tag{46}$$

where $a = 1/\delta - 1$ and $W(t)$ is the Lambert W function (the inverse of the function : $t\exp(t)$).

For the numerical test, we take $\delta = 0.0001$. We provide the solution of combustion equation by time

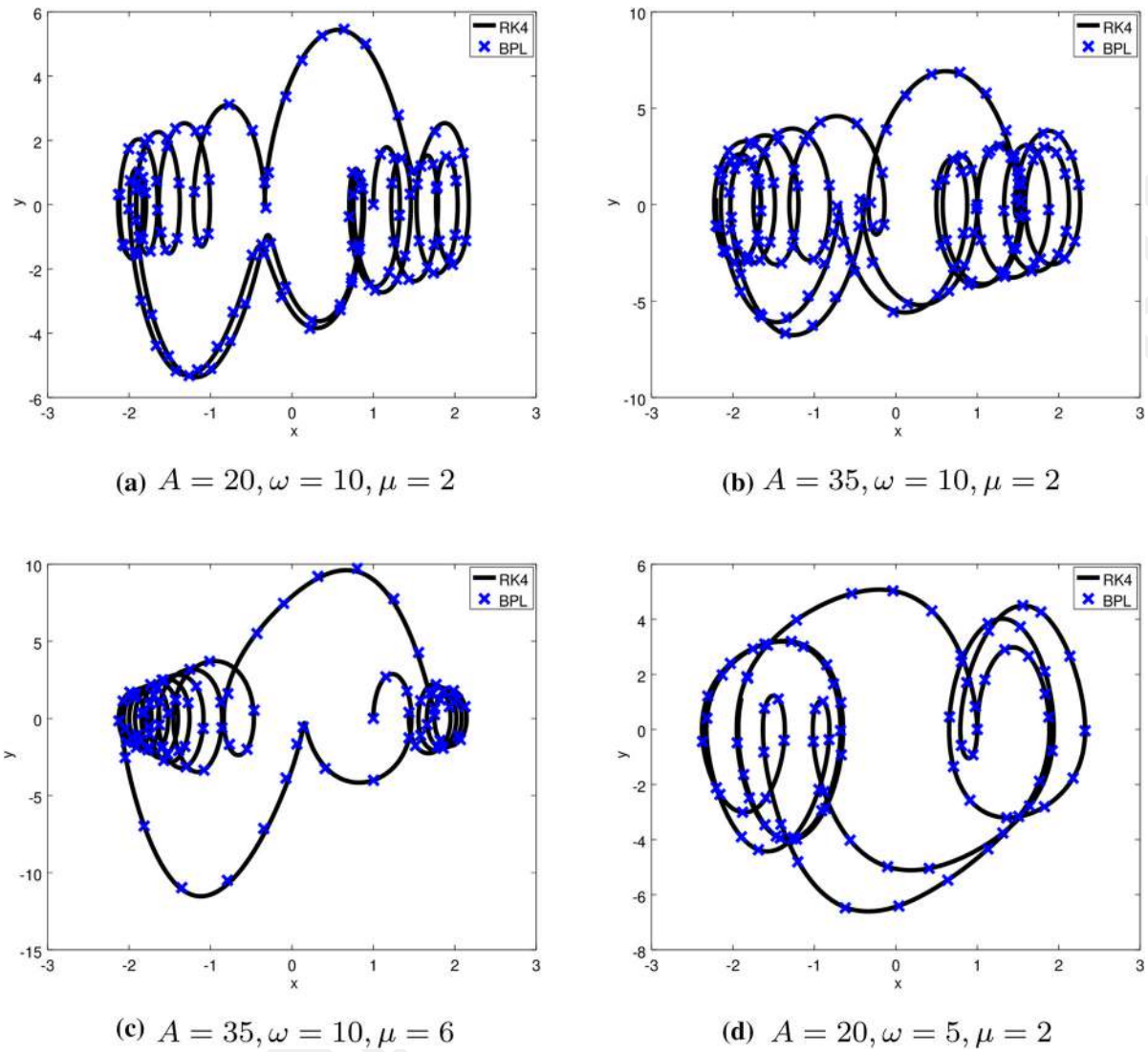

(a) $A = 20, \omega = 10, \mu = 2$ (b) $A = 35, \omega = 10, \mu = 2$

(c) $A = 35, \omega = 10, \mu = 6$ (d) $A = 20, \omega = 5, \mu = 2$

Fig. 16 Phase portrait using BPL for $\epsilon = 10^{-4}$, $N = 15$, for different values of amplitude A, frequency ω and μ, for the forced Van der Pol oscillator. In black, the reference RK4 solution using $\Delta t = 10^{-3}$s

perturbation methods and MATLAB ode solvers. We start by ode45 (based on an explicit Runge–Kutta (4, 5) formula and the Dormand–Prince pair [51]), since in general it is the best solver to apply as a first try for the majority of problems.

Figure 17 shows the exact solution compared to the solution obtained by time perturbation method and the MATLAB solver ode45 with the zoom detail, for a final time equal to $2/\delta$, so to $t = 20,000$ s. One can see that the solution obtained by the solver ode45 gives oscillatory motion, while ANM solution is in a very good agreement with the exact one. Same result as ANM is obtained by BPL and IFS.

Note that good results can be obtained with MATLAB solver ode23s (based on a modified Rosenbrock formula of order 2 [49]). However, it only solves some kinds of stiff problems and none of all ode solvers is exempt from the step size restriction. Thus, the qualitative features of the solution obtained by time perturbation method are shown.

Table 5 Case of the forced Van der Pol equation ($\mu = 2, \omega = 4$ and $A = 17$)

Tolerance	ANM	BPL	IFS
10^{-2}	53	49	74
10^{-3}	61	65	99
10^{-4}	77	79	108

Number of steps needed to reach final time $t = 10$ s using perturbation methods with $N = 15$ and different values of the residual tolerance ϵ

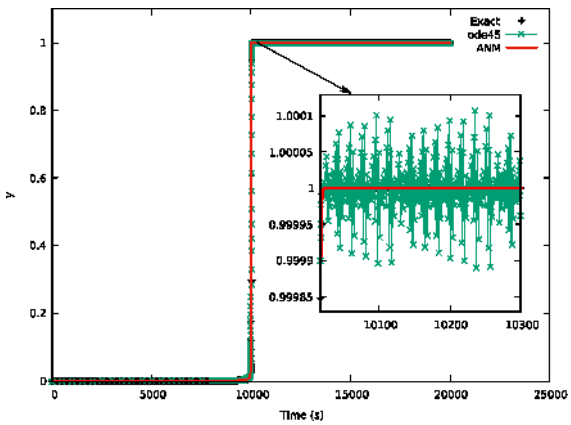

Fig. 17 Solution of Eq. (44) obtained by time perturbation method (ANM) and ode45 for $\delta = 0.0001$

6 Application on the elastic hardening spring problem

Consider the nonlinear elastic hardening spring problem [52,53] in the modified following form :

$$\ddot{u} + s_1(1 + s_2 y)u = 0 \tag{47}$$

$$y - u^2 = 0 \tag{48}$$

with the initials conditions $u(0) = u_0$, $\dot{u}(0) = v_0$, $y(0) = {u_0}^2$, where $s_1 > 0$ and $s_2 > 0$. This problem is an example of conservative systems which maintain a constant total energy in their exact solutions.

Solution of this problem presents periodic oscillations. The exact period and solution can be found analytically in [54]. Series terms of time perturbation method for Eqs. (47) and (48) are given in "Appendix C.2".

For numerical results, we take $u_0 = 1.5$, $v_0 = 0.0$, $s_1 = 100$, $s_2 = 10$ as presented in [52]. The nonlinear period of the problem is $T = 0.15153$. Classic time integration schemes use a discrete time step $\Delta T = T/32$. The phase portraits of the reference solution and the one obtained by time perturbation method (ANM) are given in Fig. 18. Same results are obtained by BPL and IFS. It is seen that good agreement is obtained. However, results obtained with classical discrete time step Δt show the inaccuracy of the numerical solution. In conservative systems, the exact displacement-velocity portrait should be a closed cycle which is not satisfied by the classical integration schemes Runge–Kutta of third (RK3) and fourth order (RK4) as can be deduced from Fig. 18. Note that similar results are obtained by using the following classical schemes: Newmark, the Houbolt method, α-method, the average acceleration method, the central difference method and the Wilson θ-method. This has been confirmed by the deviation of the total energy obtained by these schemes from its initial value in [53].

The results depicted in Fig. 18 prove that a good quality of solution is guaranteed over large period of time with time perturbation methods as explained in [20].

7 Application on a three degrees of freedom (3 DOF) example : Lorenz system

One of the most famous chaotic systems was developed by Edward Lorenz [55] who was interested in the fluid flow patterns of the Earth's atmosphere and noticed an unexpected chaotic behavior. Depending on the choice of the parameters that exist in the equations, Lorenz system can exhibit chaotic and non-chaotic behavior. The Lorenz equations govern, in a lower order, the dynamics of convection in a heated fluid layer and present particular challenges due to its high sensitivity to small variations in initial conditions, from continuous convection to low turbulence (chaos). The Lorenz equations are:

$$\dot{x} = \sigma(y - x) \tag{49}$$

$$\dot{y} = x(\rho - z) - y \tag{50}$$

$$\dot{z} = xy - \beta z \tag{51}$$

where x, y and z are dynamical variables. The first component of the solution x is related to the convection in the atmospheric flow, while the other two components y and z are related to horizontal and vertical tempera-

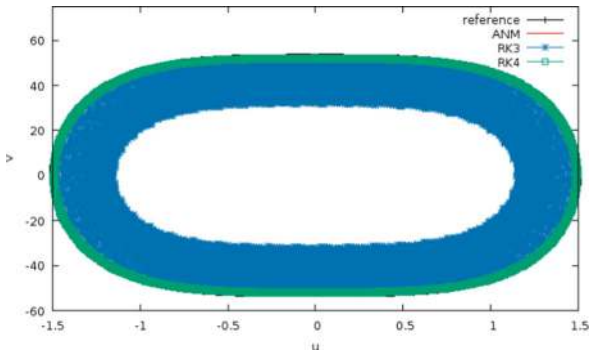

(a)

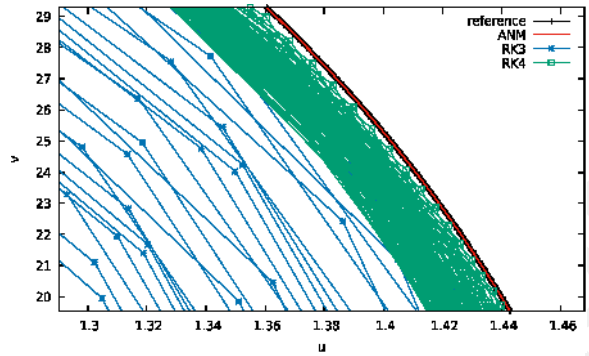

(b)

Fig. 18 Phase portraits of the hardening spring problem $\ddot{u} + 100(1 + 10u^2)u = 0$, $u_0 = 1.5$, $v_0 = 0.0$ for a final time equal to $50T$, by time perturbation method (ANM) and the third- and fourth-order Runge–Kutta method (RK3/RK4) with a discrete time step $\Delta t = T/32$. Reference solution presented in [54]. (b) is a zoom plot of (a)

ture variation. The parameters σ , ρ and β are the related constants.

Series terms of time perturbation method for this system are given in "Appendix C.3".

Note that this system of differential equations is not linear and it is very complicated to obtain exact solutions with the presence of two nonlinear terms. Solutions are completely dependent on initial parameters and conditions, and it is very difficult to predict their behavior. For some parameter values, the orbit of the solution in the three-dimensional space is a strange attractor. For other values of the parameters, the solution tends either to converge toward a fixed point, or diverge to infinity or follow a periodic oscillation motion. Bifurcation studies show that with the parameters $\sigma = 10$ and $\beta = 8/3$, and the critical chaos parameter is $\rho = \rho_{\text{cr}} = 27.74$ [56]. The behavior of the solution is non-chaotic when $\rho < \rho_{\text{cr}}$ and chaotic otherwise.

When resolving this system numerically, the numerical methods provide the solutions only at a discrete point in time. In order to ensure a good convergence of the solution, these methods require a very small discrete time step. However, even by reducing the integration step Δt, the result cannot be improved. This is due to the fact that the integration error presents an extremum as a function of Δt as mentioned in [57]. The importance of handling Lorenz system with a time perturbation method instead of a discrete time integrator is outlined in [57,58].

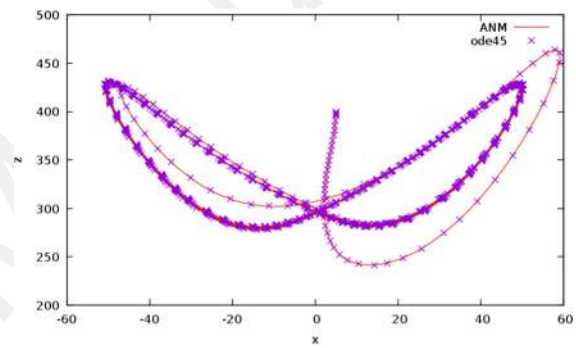

Fig. 19 Phase portraits of Lorenz system with $x_0 = 5$, $y_0 = 5$, $z_0 = 400$ and $\rho = 350$ obtained by time perturbation method (ANM) and ode45

For the numerical results, the following initials conditions are set first to $x_0 = 5$, $y_0 = 5$, $z_0 = 400$ and the constant ρ is set to $\rho = 350$. Figure 19 illustrates the phase portrait of Lorenz system and shows the efficiency of time perturbation method.

Then, we consider $x_0 = 5$, $y_0 = 5$, $z_0 = 4$ and $\rho = 27$. Figure 20 shows the ability of time perturbation methods to reproduce the Lorenz attractor.

Same results are obtained for both test cases using BPL and IFS.

8 Conclusions and perspectives

Nonlinear differential equations have been successfully solved using time perturbation methods as time

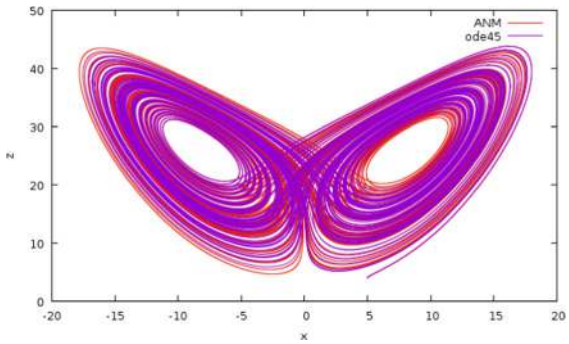

Fig. 20 Phase portraits of Lorenz system with $x_0 = 5$, $y_0 = 5$, $z_0 = 4$ and $\rho = 27$ obtained by time perturbation method (ANM) and ode45

integrator. Full description of the time perturbation has been made. First, classic Asymptotic Numerical Method has been applied using time as perturbation parameter. Then, resummation techniques Borel–Padé-Laplace and Inverse-Factorial Series have been studied. First- and second-order derivatives are explicitly given for both BPL and IFS methods. This is one of the main contributions of this work.

The principal advantage of such approaches is that solutions and derivatives are continuous in time. It makes it possible to evaluate those latter at any time. It is noted that for free and forced Van der Pol equations, both ANM and BPL methods are equivalent in terms of number of steps using proposed parameters. Time perturbation methods make it possible to perform wider time step, with a prescribed residual, than adaptive RK4 integrator. It is noted that computational efforts of classic and perturbation methods are globally in the same order of magnitude. Most of the CPU time for ANM(R), BPL and IFS is spent in the evaluation of the range of validity. An incremental algorithm is being used, where dichotomy should be much faster.

It has been confirmed that poles appear during continuation of BPL method. It is difficult to find correct parameters for BPL : truncation order, number of Gauss points, for which poles are not an issue. In this study, IFS is a bit less efficient, but it can provide a good alternative to BPL where poles might appear and in the case of divergent series, for which ANM method is no longer efficient.

Finally, time perturbation and resummation methods are well adapted to simulation over long time. Several examples have indicated that classical schemes often introduce a slight shift at each period, whereas the time perturbation schemes reproduce more faithfully the limit cycle. The efficiency of these methods has also been validated for the 3 DOF Lorenz system. Some recent studies even show that time perturbation features allow to handle correctly problems like Lorenz system.

Application to models using high numbers of degrees of freedom, more precise computational efforts and comparisons of the proposed time perturbation integrators will be studied in a further work.

Compliance with ethical standards

Conflict of interest The authors declare that they have no conflict of interest.

Appendix A Derivatives formulas for Borel–Padé–Laplace

The Borel sum denoted by $S\hat{u}(t)$ in a direction $d = \mathbb{R}^+$ is given by the following formula:

$$S\hat{u}(t) = u_0 + \int_0^\infty P(\xi) e^{-\xi/t} d\xi \tag{52}$$

The first derivative of Borel sum is given by:

$$\frac{\mathrm{d}S\hat{u}(t)}{\mathrm{d}t} = \frac{\mathrm{d}}{\mathrm{d}t}\left(u_0 + \int_0^\infty P(\xi) e^{-\xi/t} \mathrm{d}\xi\right) \tag{53}$$

$$= \frac{\mathrm{d}u_0}{\mathrm{d}t} + \int_0^\infty P(\xi) \frac{\mathrm{d}}{\mathrm{d}t}(e^{-\xi/t}) \mathrm{d}\xi \tag{54}$$

$$= 0 + \int_0^\infty P(\xi) (\frac{\xi}{t^2}) e^{-\xi/t} \mathrm{d}\xi \tag{55}$$

$$= \frac{1}{t^2} \int_0^\infty \xi P(\xi) e^{-\xi/t} d\xi \tag{56}$$

The change of variable $\xi = rt$ yields to:

$$\frac{\mathrm{d}S\hat{u}(t)}{\mathrm{d}t} = \frac{1}{t^2} \int_0^\infty rt P(\mathrm{rt}) e^{-r} \mathrm{d}(\mathrm{rt}) \tag{57}$$

$$= \frac{t^2}{t^2} \int_0^\infty r P(\mathrm{rt}) e^{-r} \mathrm{d}r \tag{58}$$

$$= \int_0^\infty r P(\mathrm{rt}) e^{-r} \mathrm{d}r \tag{59}$$

Finally, the first derivative of $S\hat{u}(t)$ is

$$\frac{\mathrm{d}S\hat{u}(t)}{\mathrm{d}t} = \int_0^\infty r P(\mathrm{rt}) e^{-r} \mathrm{d}r \tag{60}$$

The second derivative of Borel sum is given by:

$$\frac{\mathrm{d}^2 S\hat{u}(t)}{\mathrm{d}t^2} = \frac{\mathrm{d}}{\mathrm{d}t}\left(\frac{1}{t^2}\int_0^\infty \xi P(\xi) e^{-\xi/t}\mathrm{d}\xi\right) \tag{61}$$

$$= I_1 + I_2 \tag{62}$$

with

$$I_1 = \frac{\mathrm{d}}{\mathrm{d}t}(\frac{1}{t^2})\int_0^\infty \xi P(\xi) e^{-\xi/t}\mathrm{d}\xi \tag{63}$$

and

$$I_2 = \frac{1}{t^2}\frac{\mathrm{d}}{\mathrm{d}t}\int_0^\infty \xi P(\xi) e^{-\xi/t}\mathrm{d}\xi \tag{64}$$

For I_1:

$$I_1 = \frac{\mathrm{d}}{\mathrm{d}t}(\frac{1}{t^2})\int_0^\infty \xi P(\xi) e^{-\xi/t}\mathrm{d}\xi \tag{65}$$

$$= \frac{-2}{t^3}\int_0^\infty \xi P(\xi) e^{-\xi/t}\mathrm{d}\xi \tag{66}$$

Let the change of variable $\xi = rt$

$$I_1 = \frac{-2}{t^3}\int_0^\infty \mathrm{rt} P(\mathrm{rt}) e^{-r}\mathrm{d}(\mathrm{rt}) \tag{67}$$

$$= \frac{-2}{t}\int_0^\infty r P(\mathrm{rt}) e^{-r}\mathrm{d}r \tag{68}$$

$$= \frac{-2}{t}\frac{\mathrm{d}S\hat{u}(t)}{\mathrm{d}t} \tag{69}$$

Therefore,

$$I_1 = \frac{-2}{t}\frac{\mathrm{d}S\hat{u}(t)}{\mathrm{d}t} \tag{70}$$

For I_2:

$$I_2 = \frac{1}{t^2}\frac{\mathrm{d}}{\mathrm{d}t}\int_0^\infty \xi P(\xi) e^{-\xi/t}\mathrm{d}\xi \tag{71}$$

$$= \frac{1}{t^2}\int_0^\infty \xi P(\xi)\frac{\xi}{t^2} e^{-\xi/t}\mathrm{d}\xi \tag{72}$$

$$= \frac{1}{t^4}\int_0^\infty \xi^2 P(\xi) e^{-\xi/t}\mathrm{d}\xi \tag{73}$$

Let the change of variable $\xi = rt$

$$I_2 = \frac{1}{t^4}\int_0^\infty r^2 t^2 P(\mathrm{rt}) e^{-r}\mathrm{d}(\mathrm{rt}) \tag{74}$$

$$= \frac{1}{t}\int_0^\infty r^2 P(\mathrm{rt}) e^{-r}\mathrm{d}r \tag{75}$$

Therefore, the second derivative of Borel sum is

$$\frac{\mathrm{d}^2 S\hat{u}(t)}{\mathrm{d}t^2} = \frac{-2}{t}\frac{\mathrm{d}S\hat{u}(t)}{\mathrm{d}t} + \frac{1}{t}\int_0^\infty r^2 P(\mathrm{rt}) e^{-r}\mathrm{d}r \tag{76}$$

Note that the evaluation of the second derivative of Borel sum needs to start from $t_0 \neq 0$.

Therefore, as a summary:

$$S\hat{u}(t) = u_0 + t\int_0^\infty P(\mathrm{rt}) e^{-r}\mathrm{d}r \tag{77}$$

$$\frac{\mathrm{d}S\hat{u}(t)}{\mathrm{d}t} = \int_0^\infty r P(\mathrm{rt}) e^{-r}\mathrm{d}r \tag{78}$$

$$\frac{\mathrm{d}^2 S\hat{u}(t)}{\mathrm{d}t^2} = \frac{-2}{t}\frac{\mathrm{d}S\hat{u}(t)}{\mathrm{d}t} + \frac{1}{t}\int_0^\infty r^2 P(\mathrm{rt}) e^{-r}\mathrm{d}r \tag{79}$$

A quick reminder about Gauss–Laguerre quadrature is presented:

$$\int_0^\infty f(x) e^{-x}\mathrm{d}x = \sum_{i=1}^{N_G} w_i f(x_i) \tag{80}$$

with w_i are the quadrature coefficients (or weights). The x_i points, or nodes, are real, distinct, unique and are the roots of Laguerre's N_G polynomials.

Generally, we can also consider the integrals that have a singularity of the law of power x^α known to $x = 0$, for $\alpha > -1$ with α a real number that lead to integrals of forms:

$$\int_0^\infty x^\alpha f(x) e^{-x}\mathrm{d}x = \sum_{i=1}^{N_G} w_i f(x_i) \tag{81}$$

This allows to estimate such integrals accurately for $f(x)$ smooth or polynomial even in the case where α is not an integer.

It should be noticed that the nodes x_i and the weighs w_i depend on α and N_G. So, here are two different strategies for calculating first and second derivatives of BPL.

A.1 Strategy 1

Strategy 1 is an application of Gauss–Laguerre formula or the generalized formula with $\alpha = 0$.

Borel sum is given by:

$$\begin{aligned} S\hat{u}(t) &= u_0 + t\int_0^\infty \underbrace{P(\mathrm{rt})}_{H(r)} e^{-r} dr \\ &= u_0 + t\int_0^\infty H(r)e^{-r}\mathrm{d}r \\ &= u_0 + t\sum_{i=1}^{N_G} w_i H(r_i) \\ &= u_0 + t\sum_{i=1}^{N_G} w_i P(r_i t) \end{aligned} \tag{82}$$

The first derivative of Borel sum is given by:

$$\begin{aligned} \frac{\mathrm{d}S\hat{u}(t)}{\mathrm{d}t} &= \int_0^\infty \underbrace{r\,P(\mathrm{rt})}_{G(r)} e^{-r}\mathrm{d}r \\ &= \int_0^\infty G(r)e^{-r}\mathrm{d}r = \sum_{i=1}^{N_G} w_i G(r_i) \\ &= \sum_{i=1}^{N_G} w_i r_i P(r_i t) \end{aligned} \tag{83}$$

The second derivative of Borel sum is given by:

$$\begin{aligned} \frac{\mathrm{d}^2 S\hat{u}(t)}{\mathrm{d}t^2} &= \frac{-2}{t}\frac{\mathrm{d}S\hat{u}(t)}{\mathrm{d}t} + \frac{1}{t}\int_0^\infty \underbrace{r^2 P(\mathrm{rt})}_{Q(r,t)} e^{-r}\mathrm{d}r \\ &= \frac{-2}{t}\frac{\mathrm{d}S\hat{u}(t)}{\mathrm{d}t} + \frac{1}{t}\sum_{i=1}^{N_G} w_i Q(r_i, t) \\ &= \frac{-2}{t}\frac{\mathrm{d}S\hat{u}(t)}{\mathrm{d}t} + \frac{1}{t}\sum_{i=1}^{N_G} w_i {r_i}^2 P(r_i t) \end{aligned} \tag{84}$$

Therefore, with $\alpha = 0$, we have

$$S\hat{u}(t) = u_0 + t\sum_{i=1}^{N_G} w_i P(r_i t) \tag{85}$$

$$\frac{\mathrm{d}S\hat{u}(t)}{\mathrm{d}t} = \sum_{i=1}^{N_G} w_i r_i P(r_i t) \tag{86}$$

$$\frac{\mathrm{d}^2 S\hat{u}(t)}{\mathrm{d}t^2} = \frac{-2}{t}\frac{\mathrm{d}S\hat{u}(t)}{\mathrm{d}t} + \frac{1}{t}\sum_{i=1}^{N_G} w_i {r_i}^2 P(r_i t) \tag{87}$$

For this first way, the Padé solution $P(r_i t)$ is calculated only once for the estimation of the Borel solution, the first and second derivatives.

A.2 Strategy 2

The second way is based on generalized Gauss–Laguerre.

For $\alpha = 0$, we have:

$$\begin{aligned} S\hat{u}(t) &= u_0 + t\int_0^\infty \underbrace{P(\mathrm{rt})}_{H(r)} e^{-r}\mathrm{d}r \\ &= u_0 + t\int_0^\infty H(r)e^{-r}\mathrm{d}r \\ &= u_0 + t\sum_{i=1}^{N_G} w_i H(r_i) = u_0 + t\sum_{i=1}^{N_G} w_i P(r_i t) \end{aligned} \tag{88}$$

For $\alpha = 1$, we have:

$$\begin{aligned} \frac{\mathrm{d}S\hat{u}(t)}{\mathrm{d}t} &= \int_0^\infty r\,\underbrace{P(\mathrm{rt})}_{G(r)} e^{-r}\mathrm{d}r \\ &= \int_0^\infty rG(r)e^{-r}\mathrm{d}r \\ &= \sum_{i=1}^{N_G} w_i G(r_i) = \sum_{i=1}^{N_G} w_i P(r_i t) \end{aligned} \tag{89}$$

For $\alpha = 2$, we have:

$$\begin{aligned} \frac{\mathrm{d}^2 S\hat{u}(t)}{\mathrm{d}t^2} &= \frac{-2}{t}\frac{\mathrm{d}S\hat{u}(t)}{\mathrm{d}t} + \frac{1}{t}\int_0^\infty r^2 \underbrace{P(\mathrm{rt})}_{Q(r,t)} e^{-r}\mathrm{d}r \\ &= \frac{-2}{t}\frac{\mathrm{d}S\hat{u}(t)}{\mathrm{d}t} + \frac{1}{t}\int_0^\infty r^2 Q(r,t)e^{-r}\mathrm{d}r \\ &= \frac{-2}{t}\frac{\mathrm{d}S\hat{u}(t)}{\mathrm{d}t} + \frac{1}{t}\sum_{i=1}^{N_G} w_i P(r_i t) \end{aligned} \tag{90}$$

Therefore,

$$S\hat{u}(t) = u_0 + t\sum_{i=1}^{N_G} w_i P(r_i t) \qquad \alpha = 0 \tag{91}$$

$$\frac{\mathrm{d}S\hat{u}(t)}{\mathrm{d}t} = \sum_{i=1}^{N_G} w_i P(r_i t) \qquad \alpha = 1 \tag{92}$$

$$\frac{\mathrm{d}^2 S\hat{u}(t)}{\mathrm{d}t^2} = \frac{-2}{t}\frac{\mathrm{d}S\hat{u}(t)}{\mathrm{d}t} + \frac{1}{t}\sum_{i=1}^{N_G} w_i P(r_i t) \qquad \alpha = 2 \tag{93}$$

For this strategy, Padé's development is not the same for Borel sum and its derivative since the roots and the weight depend on α.

Appendix B Derivatives formulas for inverse factorial series

In this "Appendix," we calculate the first and second derivatives of Inverse factorial series $I(t)$ of the second way of Sect. 2.3 (great order N). We recall some definition of this sub-section before starting to evaluate the derivatives.

Suppose that $\hat{u}(t)$ is 1-summable in a direction d, with an angle θ with the positive half-axis. Let $\tau_l = s_l e^{i\theta}$ with $l = (1, 2, \ldots, N)$, where $\{s_1, s_2, \ldots, s_N\}$ is any sequence of complex numbers. Let

$$z = \frac{1}{t}, \qquad y = ze^{i\theta} \tag{94}$$

$$a_1 = \frac{u_0}{z}, a_2 = \frac{u_1}{z^2}, \ldots, a_m = \frac{u_{m-1}}{z^m}, \quad m = 1, \ldots \tag{95}$$

Note that if the series are summable in $\mathbb{R}^+$ direction, so $y = z$ and we will choose $s_l = l$ for $l \geq 1$.

We call Inverse factorial series the following:

$$I(t) = \frac{1}{t}\sum_{n=0}^{N-1} v_{n+1} = z\sum_{n=0}^{N-1} v_{n+1} = z(v_1 + v_2 + \cdots + v_N) \tag{96}$$

where v_n is the n-th term of IFS which is calculated using the following recursive algorithm based on

$$v_{n+1}^{(j)} = \frac{\tau_{n-1} v_n^{(j)} + y v_n^{(j+1)}}{y + \tau_n} \qquad n \geq 1, j \geq 1, \tag{97}$$

with

$$v_1^{(1)} = a_1 \qquad v_1^{(2)} = a_2 \qquad \ldots \qquad v_1^{(N)} = a_N \tag{98}$$

The terms $v_1^{(1)}, v_2^{(1)}, \ldots, v_n^{(1)}, v_{n+1}^{(1)}$ are the terms of the IFS denoted by: $v_1, v_2, \ldots, v_n, v_{n+1}$.

B.1 First derivative

Note that the derivative in this "Appendix" will be denoted by premium even if they are temporal derivatives. (Just for more clarification in the formulas).

The first derivative of Inverse factorial series is given by:

$$\frac{\mathrm{d}I(t)}{\mathrm{d}t} = I'(t) = z'(v_1 + v_2 + \cdots + v_N) + z(v_1{}' + v_2{}' + \cdots + v_N') \tag{99}$$

We have

$$z' = \frac{-1}{t^2} \tag{100}$$

We will build a recursive algorithm of derivative to evaluate $I'(t)$.

We have

$$a_m = \frac{u_{m-1}}{z^m} \implies a_m' = \frac{-m u_{m-1} z'}{z^{m+1}} \tag{101}$$

This algorithm for $n \geq 1$ is based on

$$(v_{n+1}^{(j)})' = \frac{\left(\tau_{n-1}(v_n^{(j)})' + y' v_n^{(j+1)} + y(v_n^{(j+1)})'\right)(y + \tau_n) - y'\left(\tau_{n-1} v_n^{(j)} + y v_n^{(j+1)}\right)}{(y + \tau_n)^2} \tag{102}$$

with $\tau_0 = 0$ and

$$(v_1^{(i)})' = a_i' \quad i \geq 1 \tag{103}$$

and

$$y' = z' e^{i\theta} \tag{104}$$

If the series are summable in the $\mathbb{R}^+$ direction, so

$$y' = z' \tag{105}$$

The terms $(v_1^{(1)})', (v_2^{(1)})', \ldots, (v_n^{(1)})', (v_{n+1}^{(1)})' \ldots$ are the terms of the D_{IFS}, (first derivative terms of IFS) : $v_1', v_2', \ldots, v_n', v_{n+1}'$.

B.2 Second derivative

The second derivative of Inverse factorial series is given by:

$$\begin{aligned}\frac{\mathrm{d}^2 I(t)}{\mathrm{d}t^2} =& I''(t) = z''(v_1 + v_2 + \cdots + v_{N+1}) \\ &+ 2z'(v_1' + v_2' + \cdots + v'_{N+1}) \\ &+ z(v_1'' + v_2'' + \cdots + v''_{N+1})\end{aligned} \tag{106}$$

We have

$$z'' = \frac{2}{t^3} \tag{107}$$

and

$$\begin{aligned}a_m' &= \frac{-mu_{m-1}z'}{z^{m+1}} \implies a_m'' \\ &= \frac{-mu_{m-1}\left(z''z^{m+1} - (m+1)z^m z'^2\right)}{z^{2(m+1)}}\end{aligned} \tag{108}$$

We will build a recursive algorithm of second derivative. Since the second derivative is complicated to write it directly, we will evaluate it using A, B, C such that

$$A = \left(\tau_{n-1}(v_n^{(j)})' + y'v_n^{(j+1)} + y(v_n^{(j+1)})'\right)(y + \tau_n) \tag{109}$$

and

$$B = -y'(\tau_{n-1}v_n^{(j)} + yv_n^{(j+1)}) \tag{110}$$

and

$$C = (y + \tau_n)^2 \tag{111}$$

So

$$(v_{n+1}^{(j)})'' = \frac{(A' + B')C - C'(A + B)}{C^2} \tag{112}$$

with

$$\begin{aligned}A' =& \left(\tau_{n-1}(v_n^{(j)})'' + y''v_n^{(j+1)} + y'(v_n^{(j+1)})'\right. \\ &\left. + y'(v_n^{(j+1)})' + y(v_n^{(j+1)})''\right)(y + \tau_n) \\ &+ y'\left(\tau_{n-1}(v_n^{(j)})' + y'v_n^{(j+1)} + y(v_n^{(j+1)})'\right)\end{aligned} \tag{113}$$

and

$$\begin{aligned}B' =& -y''\left(\tau_{n-1}v_n^{(j)} + yv_n^{(j+1)}\right) \\ &- y'\left(\tau_{n-1}(v_n^{(j)})' + y'v_n^{(j+1)} + y(v_n^{(j+1)})'\right)\end{aligned} \tag{114}$$

and

$$C' = 2(y + \tau_n)y' \tag{115}$$

with

$$(v_1^{(i)})'' = a_i'' \quad i \geq 1 \tag{116}$$

with

$$y'' = z''e^{i\theta} \tag{117}$$

If the series are summable in the $\mathbb{R}^+$ direction, so

$$y'' = z'' \tag{118}$$

The terms $(v_1^{(1)})'', (v_2^{(1)})'', \ldots, (v_n^{(1)})'', (v_{n+1}^{(1)})''$ are the terms of the D^2_{IFS}, (second derivative terms of IFS) : $v_1'', v_2'', \ldots, v_n'', v_{n+1}''$.

Appendix C Series terms for time perturbation methods

C.1 Nonlinear combustion equation

The nonlinear combustion equation is

$$\dot{y} = y^2(1 - y) \tag{119}$$

For sake of recurrence formulas, it is recast as follows

$$\dot{y} - z(1 - y) = 0 \tag{120}$$

$$z - y^2 = 0 \tag{121}$$

Series terms for $k \geq 1$ for Eqs. (120) and (121) are given by the following recurrence formulas:

$$ky_k = -\sum_{i=0}^{k-1} z_i y_{k-1-i} \tag{122}$$

$$z_i = \sum_{j=0}^{i} y_j y_{i-j} \tag{123}$$

C.2 Elastic hardening spring problem

The nonlinear elastic hardening spring problem is in the form

$$\ddot{u} + s_1(1 + s_2 y)u = 0 \tag{124}$$

$$y - u^2 = 0 \tag{125}$$

Series terms for equations (124) and (125) for $k \geq 2$ are given by the following recurrence formulas:

$$k(k-1)u_k = -s_1 \left(\sum_{i=0}^{k-2} (1 + s_2 y_i) u_{k-2-i} \right) \tag{126}$$

$$y_i = \sum_{j=0}^{i} u_j u_{i-j} \tag{127}$$

C.3 Lorenz attractor

The Lorenz equations are

$$\dot{x} = \sigma(y - x) \tag{128}$$

$$\dot{y} = x(\rho - z) - y \tag{129}$$

$$\dot{z} = xy - \beta z \tag{130}$$

Series terms for Lorenz equations for $k \geq 1$ are given by the following recurrence formulas:

$$x_k = \frac{1}{k} \sigma \left(y_{k-1} - x_{k-1} \right) \tag{131}$$

$$y_k = \frac{1}{k} \left(\rho x_{k-1} - \sum_{i=0}^{k-1} x_i z_{k-1-i} - y_{k-1} \right) \tag{132}$$

$$z_k = \frac{1}{k} \left(\sum_{i=0}^{k-1} x_i y_{k-1-i} - \beta z_{k-1} \right) \tag{133}$$

References

1. Fafard, M., Henchi, K., Gendron, G., Ammar, S.: Application of an asymptotic method to transient dynamic problems. J. Sound Vib. **208**(1), 73–99 (1997)
2. Razafindralandy, D., Hamdouni, A.: Time integration algorithm based on divergent series resummation, for ordinary and partial differential equations. J. Comput. Phys. **236**, 56–73 (2013)
3. Allery, C., Guerin, S., Hamdouni, A., Sakout, A.: Experimental and numerical POD study of the Coanda effect used to reduce self-sustained tones. Mech. Res. Commun. **31**(1), 105–120 (2004)
4. Boumediene, F., Miloudi, A., Cadou, J.M., Duigou, L., Boutyour, E.H.: Nonlinear forced vibration of damped plates by an asymptotic numerical method. Comput. Struct. **87**(23), 1508–1515 (2009)
5. Boutyour, E.H., Zahrouni, H., Potier-Ferry, M., Boudi, M.: Asymptotic-numerical method for buckling analysis of shell structures with large rotations. J. Comput. Appl. Math. **168**(1), 77–85 (2004)
6. Cadou, J.M., Potier-Ferry, M., Cochelin, B.: A numerical method for the computation of bifurcation points in fluid mechanics. Eur. J. Mech. B/Fluids **25**(2), 234–254 (2006)
7. Cadou, J.M., Potier-Ferry, M., Cochelin, B., Damil, N.: ANM for stationary Navier–Stokes equations and with Petrov–Galerkin formulation. Int. J. Numer. Methods Eng. **50**(4), 825–845 (2001)
8. Daya, E.M., Potier-Ferry, M.: A numerical method for nonlinear eigenvalue problems application to vibrations of viscoelastic structures. Comput. Struct. **79**(5), 533–541 (2001)
9. Guevel, Y., Boutyour, H., Cadou, J.M.: Automatic detection and branch switching methods for steady bifurcation in fluid mechanics. J. Comput. Phys. **230**(9), 3614–3629 (2011)
10. Medale, M., Cochelin, B.: A parallel computer implementation of the asymptotic numerical method to study thermal convection instabilities. J. Comput. Phys. **228**(22), 8249–8262 (2009)
11. Braikat, B., Jamal, M., Damil, N.: A high order continuation based on time power series expansion and time rational representation for solving nonlinear structural dynamic problems. Int. J. Res. Eng. Sci. **1**(6), 29–34 (2013)
12. Deeb, A.: Intégrateurs temporels basés sur la resommation des séries divergentes. Application en mécanique. PhD thesis, Université de la Rochelle, 17 december (2015)
13. Razafindralandy, D.: Contribution à l'étude mathématique et numérique de la simulation des grandes échelles. PhD thesis, Université de la Rochelle, (2005)
14. Costin, O.: On Borel summation and Stokes phenomena for rank one nonlinear systems of ODE's. Duke Math. J. **93**, 289 (1998)
15. Lutz, D.A., Miyake, M., Schäfke, R.: On the Borel summability of divergent solutions of the heat equation. Nagoya Math. J. **154**, 1 (1999)
16. Lysik, G.: Borel summable solutions of the Burgers equation. Ann. Polonici Math. **95**, 187 (2009)
17. Michalik, S.: Summability of formal solutions to the n-dimensional inhomogeneous heat equation. J. Math. Anal. Appl. **347**, 323 (2008)
18. Deeb, A., Hamdouni, A., Liberge, E., Razafindralandy, D.: Borel–Laplace summation method used as time integration scheme. ESAIM Proc. Surv. **45**, 318 (2014)
19. Razafindralandy, D., Hamdouni, A., Allery, C.: Numerical divergent series resummation in fluid flow simulation. Eur. J. Comput. Mech. **17**(4), 431–451 (2008)

20. Razafindralandy, D., Salnikov, V., Hamdouni, A., Deeb, A.: Some robust integrators for large time dynamics. Adv. Model. Simul. Eng. Sci. **6**(1), 5 (2019)
21. Razafindralandy, D., Hamdouni, A., Deeb, A.: Considering inverse factorial series as time integration method. AIP Conf. Proc. **1798**(1), 020129 (2017)
22. Davis, R.T., Alfriend, K.T.: Solutions to Van der Pol's equation using a perturbation method. Int. J. Non Linear Mech. **2**(2), 153–162 (1967)
23. Khan, MdM-U-R: Analytical solution of Van der Pol's differential equation using homotopy perturbation method. J. Appl. Math. Phys. **07**, 1–12 (2019)
24. Kimiaeifar, A., Saidi, A.R., Bagheri, G.H., Rahimpour, M., Domairry, D.G.: Analytical solution for Van der Polduffing oscillators. Chaos Solitons Fractals **42**(5), 2660–2666 (2009)
25. Saadi, H.B.: Méthodes asymptotiques-numériques pour le calcul de bifurcations de Hopf et de solutions periodiques. PhD thesis, Université de Metz, (1995)
26. Öziş, T., Yıldırım, A.: A note on He's homotopy perturbation method for Van der Pol oscillator with very strong nonlinearity. Chaos Solitons Fractals **34**(3), 989–991 (2007)
27. Parlitz, U., Lauterborn, W.: Period-doubling cascades and devil's staircases of the driven Van der Pol oscillator. Phys. Rev. A **36**, 1428–1434 (1987)
28. Cooper, M., Heidlauf, P., Sands, T.: Controlling chaos–forced Van der Pol equation. Mathematics **5**, 70 (2017)
29. Dadfar, M.B., Geer, J.F.: Resonances and power series solutions of the forced Van der Pol oscillator. SIAM J. Appl. Math. **50**(5), 1496–1506 (1990)
30. Fay, T.H.: The forced Van der Pol equation. Int. J. Math. Educ. Sci. Technol. **40**(5), 669–677 (2009)
31. Guckenheimer, J., Hoffman, K., Weckesser, W.: The forced Van der Pol equation I: the slow flow and its bifurcations. Soc. Ind. Appl. Math. **2**, 1–35 (2003)
32. Hinvi, L.A., Monwanou, A.V., Chabi Orou, J.B.: A study of the forced Van der Pol generalized oscillator with the renormalization group method. Appl. Phys. Res. **5**(6), (2013)
33. Zaripov, R.: Self-organization in the Van der Pol generator for nonextensive systems. Tech. Phys. **54**, 165–169 (2009)
34. Cochelin, B.: A path-following technique via an asymptotic-numerical method. Comput. Struct. **53**(5), 1181–1192 (1994)
35. Baguet, S.: Stability of thin-shell structures and imperfection sensitivity analysis with the asymptotic numerical method. PhD thesis, Université de la Méditerranée - Aix-Marseille II, (2001)
36. Borel, E.: Mémoire sur les séries divergentes. Annales scientifiques de l'E.N.S. 3ème série, **16**, 9 (1899)
37. Malgrange, B., Ramis, J.-P.: Fonctions multisommables. Annales de l'Institut Fourier **42**, 353 (1992)
38. Malgrange, B., Ramis, J.-P.: Fonctions multisommables. Annales de l'Institut Fourier **42**, 353 (1992)
39. Ramis, J.-P.: Séries divergentes et théories asymptotiques. Journées X-UPS 1991, page 7, (1991)
40. Guo liang Xu and Adhemar Bultheel: Matrix Padé approximation: definitions and properties. Linear Algebra Its Appl. **137–138**, 67–136 (1990)
41. Thomann, J.: Procédés formels et numériques de sommation de séries solutions d'équations différentielles. Journées X-UPS **1991**(91), 101–114 (1991)
42. Kzaz, M.: Convergence acceleration of the Gauss–Laguerre quadrature formula. Appl. Numer. Math. **29**(2), 201–220 (1999)
43. Thomann, J.: Resommation des series formelles. solutions d'équations différentielles linéaires ordinaires du second ordre dans le champ complexe au voisinage de singularités irrégulières. Numerische Mathematik **58**, 503–536 (1990)
44. Marios, T.: Theoretical and Numerical Study of the Van der Pol equation. PhD thesis, Aristotle University of Thessaloniki School of Sciences, Department of Physics, (2006)
45. Press, William H., Teukolsky, Saul A.: Adaptive stepsize Runge–Kutta integration. Comput. Phys. **6**(2), 188 (1992)
46. Cartwright, J., Piro, O.: The dynamics of Runge–Kutta methods. Int. J. Bifurc. Chaos **02**, 427–449 (1992)
47. Guillot, L., Cochelin, B., Vergez, C.: A Taylor series-based continuation method for solutions of dynamical systems. Nonlinear Dyn. **98**, 2827–2845 (2019)
48. Abelman, S., Patidar, K.: Comparison of some recent numerical methods for initial-value problems for stiff ordinary differential equations. Comput. Math. Appl. **55**, 733–744 (2008)
49. Shampine, Lawrence, Reichelt, Mark: The MATLAB ODE suite. SIAM J. Sci. Comput. Soc. Ind. Appl. Math. **18**, 1–22 (1997)
50. The Math Works. http://www.mathworks.com
51. Dormand, J.R., Prince, P.J.: A family of embedded Runge–Kutta formulae. J. Comput. Appl. Math. **6**(1), 19–26 (1980)
52. Wooram, K.I.M.: Higher-order explicit time integration methods for numerical analyses of structural dynamics. Latin Am. J. Solids Struct. **16**, 733–744 (2019)
53. Liu, Jian, Wang, Xinwei: An assessment of the differential quadrature time integration scheme for nonlinear dynamic equations. J. Sound Vib. **314**(1), 246–253 (2008)
54. Wood, W.L., Oduor, M.E.: Stability properties of some algorithms for the solution of nonlinear dynamic vibration equations. Commun. Appl. Numer. Methods **4**(2), 205–212 (1988)
55. Lorenz, Edward N.: Deterministic nonperiodic flow. J. Atmos. Sci. **20**(2), 130–141 (1963)
56. Kharchenko, V.O., Belekolos, E.D., Kharchenko, D.O.: Chaos in a generalized Lorenz system. Chaos Solitons Fractals **41**(5), 2595–2605 (2009)
57. Lozi, René, Pogonin, Vasiliy A., Pchelintsev, Alexander N.: A new accurate numerical method of approximation of chaotic solutions of dynamical model equations with quadratic nonlinearities. Chaos Solitons Fractals **91**, 108–114 (2016)
58. Lozi, René, Pchelintsev, Alexander: A new reliable numerical method for computing chaotic solutions of dynamical systems: the Chen attractor case. Int. J. Bifurc. Chaos **25**, 1550187 (2015)